

JAAP PEDERSEN¹, JANN MICHAEL WEINAND², CHLOI SYRANIDOU³
DANIEL REHFELDT⁴

An efficient solver for multi-objective onshore wind farm siting and network integration

¹  0000-0003-4047-0042
²  0000-0003-2948-876X
³  0000-0002-3332-6635
⁴  0000-0002-2877-074X

Zuse Institute Berlin
Takustr. 7
14195 Berlin
Germany

Telephone: +49 30 84185-0
Telefax: +49 30 84185-125

E-mail: bibliothek@zib.de
URL: <http://www.zib.de>

ZIB-Report (Print) ISSN 1438-0064
ZIB-Report (Internet) ISSN 2192-7782

An efficient solver for multi-objective onshore wind farm siting and network integration

Jaap Pedersen^{1,a}, Jann Michael Weinand^{2,b}, Chloi Syranidou^{3,b}, and Daniel Rehfeldt^{4,a}

^aZuse Institute Berlin, Berlin, Germany

^bForschungszentrum Jülich GmbH, Institute of Energy and Climate Research – Techno-economic Systems Analysis (IEK-3), 52425 Jülich, Germany

April 19, 2023

Abstract

Existing planning approaches for onshore wind farm siting and network integration often do not meet minimum cost solutions or social and environmental considerations. In this paper, we develop an approach for the multi-objective optimization of turbine locations and their network connection using a Quota Steiner tree problem. Applying a novel transformation on a known directed cut formulation, reduction techniques, and heuristics, we design an exact solver that makes large problem instances solvable and outperforms generic MIP solvers. Although our case studies in selected regions of Germany show large trade-offs between the objective criteria of cost and landscape impact, small burdens on one criterion can significantly improve the other criteria. In addition, we demonstrate that contrary to many approaches for exclusive turbine siting, network integration must be simultaneously optimized in order to avoid excessive costs or landscape impacts in the course of a wind farm project. Our novel problem formulation and the developed solver can assist planners in decision making and help optimize wind farms in large regions in the future.

Keywords

OR in energy, combinatorial optimization, multiple objective programming, quota Steiner tree problem, graph theory

1 Introduction

The deployment of low-carbon technologies is vital in order to mitigate climate change. As part of the transformation of the global energy system, low-cost wind energy has become an established source of electricity [1]. Between 2000 and 2019, global wind turbine capacity increased by more than 20% annually [2], reaching 730 GW in 2020 [3], with a further increase of 50% anticipated by the end of 2023 [2]. Experts also predict a sharp decline in the already low cost of wind energy by 2050 [4–6].

In recent years, however, the expansion of onshore wind has stalled in some countries and regions [7]. Despite general approval, local interest groups increasingly oppose the construction of onshore wind turbines [8–10], especially if they are not involved in the planning process [11,

¹  0000-0003-4047-0042, corresponding author, pedersen@zib.de

²  0000-0003-2948-876X

³  0000-0002-3332-6635

⁴  0000-0002-2877-074X

12]. One of the main reasons for this opposition is the visual impact of these installations on the landscape [13–17]. This opposition is most pronounced against placement of wind turbines in landscapes of high aesthetic/scenic quality, whereas wind turbines placed in less attractive landscapes are more likely to be accepted [16]. The impact of resistance is particularly evident in Germany, the country with the third-largest onshore wind capacity [18] (around 58 GW in 2022 [19]) and the fourth largest share of onshore wind in electricity generation worldwide (around 26%, [20]). After record years in 2014 and 2017, with capacity additions of 4.8 GW and 5.3 GW, respectively, only 1.0 GW, 1.4 GW, 1.6 GW and 2.4 GW of new capacity was added in 2019, 2020, 2021 and 2022 [19, 21], respectively. The rapid expansion and development of onshore wind turbines has triggered an increase in local protest movements and lawsuits across the country [22, 23]. Together with the hurdles erected by legislators for new wind turbines, this raises doubts as to whether the government’s expansion target of an additional minimum of 57 GW by 2030 is feasible [19].

In the case of larger onshore wind farms, overhead lines are usually used for grid connection, which has also led to social opposition due to the accompanying modification of the landscape [8, 24]. Even the typically used underground cables can have a negative impact on the landscape, e.g. via the cutting of paths and protective strips in forests [25]. Furthermore, historical wind energy projects have made it apparent that grid operators often implement suboptimal grid connection plans. Although grid operators are obliged under the German Renewable Energy Sources Act to establish the most economically-favorable connection points, this is rarely the case in reality [26]. A planning approach for turbine location and grid connection planning that would optimally take into account the central target criteria of cost efficiency and landscape impact could accelerate onshore wind expansion again and so support the achievement of expansion targets.

1.1 Existing literature

Recent research studies have dealt with the optimal siting of onshore wind turbines using multi-criteria objectives: in Weinand et al. [27], Lehmann et al. [28] and Tafarte & Lehmann [29], optimal onshore wind sites were determined for the entirety of Germany on the basis of the turbine levelized cost of electricity in €/MWh, aesthetic qualities of landscapes or disamenities for the inhabitants living close to them. In Weinand et al. [30], these analyses were extended to turbine siting across Europe, with a simulation rather than an optimization approach being taken due to the large number of turbines and scenarios. In these large-scale studies, grid integration is typically neglected due to the high complexity of the resulting combinatorial problem [31]. According to the results of the grid integration heuristic for onshore wind turbines discussed in McKenna et al. [32], however, the total costs are doubled on average when grid integration is taken into account. It is therefore imperative to include grid integration. Due to the complexity of the problem, grid connection planning is mostly formulated as a minimum spanning tree (MST) problem (e.g. [33]), is mostly solved heuristically [34–37], and turbine locations are specified as fixed (e.g. [38, 39]).

There are some promising examples for the design and cable routing of offshore wind farms [40, 41], but typically a fixed number of turbines are determined prior to cable routing. These studies also include some Steiner nodes to provide for more flexibility for the routing problem, which is sufficient in an offshore environment and a single wind farm. This has, however, limitations when considering onshore and multiple wind farms at the same time. In Fischetti & Fischetti [42], a combined layout and cable routing problem is discussed again in the context of offshore wind farms. The problem is modeled as a mixed-integer linear program, which is then improved by using cutting techniques. Even though the model can handle a variable set of wind turbines, it was decided to fix the number, as is done in practice of single wind farm design. In the latter articles [40–42], a single offshore wind farm is designed, and so a model formulated, that captures the technical details on graphs with 50 - 100 nodes.

An efficient way to solve the problem for larger instances is to reduce the level of technical detail, e.g., ignoring cable losses or capacity constraints on substations, etc. In this study, the problem of choosing a subset of possible wind turbines, including cable routing, is modeled

as a variant of the Steiner tree problem (STP), a generalization of the MST problem. The STP is a classic NP-hard problem [43], and one of the most studied problems in combinatorial optimization [44]. Given an undirected graph with non-negative edge costs, the STP aims to find a tree that interconnects a given set of special points (referred to as terminals) at minimum total cost. The STP and its variations arise in many real-world applications like network design problems in telecommunication, electricity, or in district heating, as well as other fields such as biology; see, e.g., Leitner et al. [45], Bolukbasi & Kocaman [46], Ljubic et al. [47], and Klimm et al. [48], respectively. A vast amount of literature concerning STP and related problems exists and for a comprehensive overview of the topic, the reader is referred to the recent survey [44]. In the context of wind farm design, the STP appears for example in the PhD thesis by Ridremont [49], in which a robust cable network is designed; again, the method is only applied on networks with up to 100 nodes and 300 edges.

In general, network design problems consist of two parts: first, a subset of profitable customers must be selected, and second, a network must be designed to connect all chosen customers with the least cost. The trade-off between maximizing profits and minimizing costs can be modeled as a generalized version of the STP: the Prize-Collecting Steiner Tree Problem (PCSTP). However, in the transition towards a carbon-neutral energy system only focusing on this trade-off is insufficient. For example, network operators must assure security of demand, there are expansion targets to be met, or a region strives to cover its demand by locally operated renewable energy sources. These additional constraints can be modeled in a generalized version of the PCSTP, namely the quota PCSTP (QSTP), with the objective of minimizing costs while a minimum amount of "profits" is collected.

Although a wide range of literature discusses the PCSTP from both the theoretical as well as the practical point of view (see the surveys in [50] and [44]), few studies have addressed the QSTP. The QSTP was initially formulated by Johnson et al. [51], who observed that it is a generalized version of the k minimum spanning tree (k -MST) problem, in which, given an edge-weighted graph G , a minimum costs subtree of G containing at least k vertices is constructed. The authors also propose a heuristic approach to solving the QSTP by introducing an increasing profit-multiplier α , and solving a series of PCSTP instances. In each iteration, a new instance is constructed by multiplying the original profits by the increased α until the quota is fulfilled. This approach results in a trade-off curve that shows which quota can be collected at which prize. Drawbacks of this approach include the fact that multiple problems must be solved and it might not be clear how to choose α , especially if costs and profits are not comparable, e.g., costs vs. energy potential; finally, the desired quota might not be captured in the trade-off curve. Haouari & Siala [52] propose a hybrid Lagrangian genetic algorithm to compute lower and upper bounds for QSTP instances with up to 5000 edges. A robust version of the QSTP was introduced in Alvarez-Miranda et al. [53]. However, the authors only discuss a branch-and-cut approach for the robust PCSTP and its budget-constrained variant and not for the QSTP. Although a number of studies on exact solution approaches for the PCSTP have been conducted so far (e.g., [47, 54, 55]), to the best of our knowledge no exact solution approach for the QSTP has been suggested in the literature.

1.2 Contribution and structure

In this study, we develop a planning instrument based on the Steiner tree approach, which is applicable to any region in Germany. This research is interdisciplinary and combines mathematical, landscape planning and energy management methods. In contrast to studies on offshore wind farm planning [40–42], our multi-objective approach aims to solve onshore wind turbine placements and cable routing on a regional level, resulting in much larger instances as a larger number of turbines are considered and more Steiner nodes are needed to assure flexibility in the cable routing. In Section 2, we first present the QSTP as a directed cut formulation. Then, we introduce a new transformation for the problem and prove the equivalence with the original formulation. We integrate both formulations into the exact Steiner tree solver SCIP-JACK [56]. We further implement a shortest-path-based reduction technique and a primal heuristic for the QSTP. Subsequently, we apply our new methodological approaches

in Section 3 to demonstrate the significant performance improvements compared to standard solvers and to demonstrate the trade-offs between cost and landscape impacts in onshore wind farm planning for several German regions. Thereby, we highlight what previous (national) planning approaches must improve, before discussing and concluding our methods and results in Section 4.

2 Quota Steiner tree problem

The Quota Steiner tree problem (QSTP) is defined, similarly to Johnson et al. [51] with the addition of vertex costs, as follows: given an undirected graph $G = (V, E)$, a set of fixed terminals $T_f \subset V$ and a set of potential terminals $T_p \subset V$ with $T_f \cap T_p = \emptyset$, where each edge $(i, j) \in E$ is associated with costs $c : E \rightarrow \mathbb{R}_{\geq 0}$, and each potential terminal $v \in T_p$ with costs $w : T_p \rightarrow \mathbb{R}_{> 0}$ and quota profits $q : T_p \rightarrow \mathbb{R}_{> 0}$. The goal is to find a tree $S = (E', V') \subseteq G$ that contains all terminals T_f such that the total cost:

$$C(S) = \sum_{(i,j) \in E'} c_{ij} + \sum_{i \in T_p \cap V'} w_i \quad (1)$$

is minimized and a given quota $Q \in \mathbb{R}_{> 0}$ is fulfilled, i.e.:

$$Q(S) = \sum_{i \in T_p \cap V'} q_i \geq Q \quad (2)$$

2.1 Directed cut formulation

The QSTP is modeled as an Steiner arborescence problem (SAP) in an integer linear program (IP). For the general SAP see e.g. Wong [57]. The original undirected graph G is transformed into a directed graph $D = (V, A)$ where $A := \{(i, j), (j, i) | \forall (i, j) \in E\}$. By applying the idea of shifting the costs of a vertex v onto the costs of its incoming arcs (see Ljubic et al. [47]), the arc costs $c : A \rightarrow \mathbb{R}_{\geq 0}$ are defined as:

$$c(i, j) = \begin{cases} c_e + w_j & \text{if } j \in T_p, \\ c_e & \text{otherwise} \end{cases} \quad \forall a = (i, j) \in A \quad (3)$$

where c_e represents the cost of the corresponding edge $e = (i, j)$ in the original undirected graph G . For a subset of nodes $W \subset V$, we denote $\delta^+(W) = \{(i, j) \in A : i \in W, j \in V \setminus W\}$ as the set of outgoing arcs and $\delta^-(W) = \{(i, j) \in A : i \in V \setminus W, j \in W\}$ as the set of incoming arcs. For a single vertex v_i , we write $\delta^+(\{v_i\}) = \delta^+(v_i)$ and $\delta^-(\{v_i\}) = \delta^-(v_i)$. For any set M , we define $x(M) = \sum_{i \in M} x_i$.

We introduce a binary variable x_{ij} for each $(i, j) \in A$ if the arc (i, j) is contained in the Steiner tree ($x_{ij} = 1$) or not ($x_{ij} = 0$). Furthermore, let y_k be a binary variable for each $k \in T_p$ indicating whether or not the potential terminal k is chosen. The rooted directed cut integer programming formulation (IP) of the QSTP with an arbitrary root $r \in T_f$ is given as follows:

$$\min \quad c^T x \quad (4)$$

s.t.

$$x(\delta^-(W)) \geq 1 \quad \forall W \subset V, r \notin W, |W \cap T_f| \geq 1 \quad (5)$$

$$x(\delta^-(W)) \geq y_i \quad \forall W \subset V, r \notin W, |W \cap T_p| \geq 1, i \in T_p \quad (6)$$

$$\sum_{i \in T_p} q_i y_i \geq Q \quad (7)$$

$$x_{ij}, y_k \in \{0, 1\} \quad \forall (i, j) \in A, \forall k \in T_p \quad (8)$$

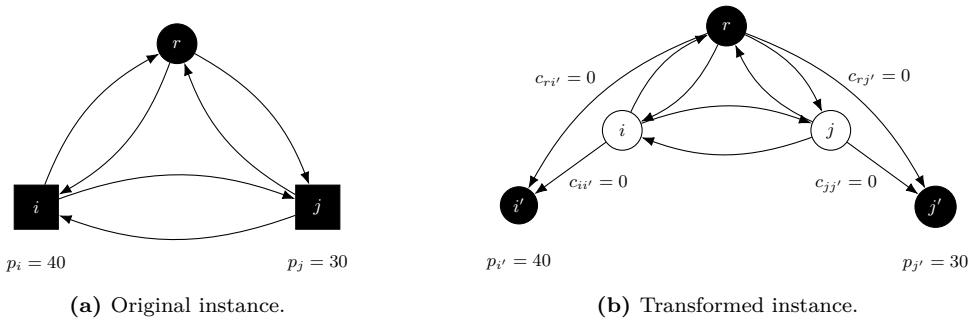


Figure 1: Transformation of QSTP. For each potential terminal $i \in T_p$ (black squares) a real terminal (black circle) i' is added with profit $q_{i'} = q_i$, which is connected to the root node r and the original vertex by an arc of zero costs. The original potential terminal $i \in T_p$ is removed from the set of potential terminals and considered a Steiner node (white circle) from here on. The original arc costs are omitted.

The constraint (5) guarantees that there exists a path from r to each $t \in T_f$ and (6) that there exists a path from r to the potential terminal $i \in T_p$ if it is chosen to contribute to the quota constraint (7). Let $I_Q = (V, A, T_f, T_p, c, q, Q)$ denote an instance of the QSTP. Note a simple observation for the QSTP:

Observation 2.1. *Considering an instance $I_Q = (V, A, T_f, T_p, c, q, Q)$ of the QSTP, if*

$$Q \geq \sum_{i \in T_p} q_i - \min_{i \in T_p} q_i$$

then the QSTP reduces to the STP by defining the set of terminals $T = T_f \cup T_p$.

2.1.1 Transformation

One of the essential features of the existing, state-of-the-art SCIP-JACK framework is the cut separation algorithm for the SAP. However, the binary variables introduced for all potential terminals prevent the direct use of this separation algorithm for the QSTP formulation presented in the previous section. Therefore, we present a transformation allowing us to solve the problem using the separation algorithm of SCIP-JACK without further adjustments.

For each potential terminal $t_i \in T_p$, a new fixed terminal t'_i with a profit of $q_{t'_i} = q_{t_i}$ is added. Furthermore, for each newly-added terminal t'_i , an arc (r, t'_i) with costs $c(r, t'_i) = 0$ and an arc (t_i, t'_i) with costs $c(t_i, t'_i) = 0$ are added. Finally, each original potential terminal $t_i \in T_p$ now becomes a Steiner node i in the transformed graph. Let T'_f be the set of the newly-added terminals and $T' = T_f \cup T'_f$ the set of all terminals in the transformed graph.

Now, if we tried to keep the structure of the quota constraint (7), the quota profit $q_{t'_i}$ would be collected if the newly-added fixed terminal t'_i is reached by the arc (t_i, t'_i) . However, by adding a constraint of form $b^T x \geq d$ with $b \in \mathbb{R}_{\geq 0}^A$ and $b \neq \mathbf{0}$ and $d \in \mathbb{R}$ to the general SAP formulation, we can no longer guarantee the connectivity of the solution, which will be explained in the following. Let us consider only the Steiner cut constraints (5). As Goemans & Myung [58] point out, the convex hull of all $x \in \mathbb{Z}_{\geq 0}^A$ satisfying these constraints is of blocking type, i.e., its recession cone consists of all non-negative vectors. This means any solution feasible for (5) can be extended by increasing x_a for any $a \in A$ and still be feasible. Only if we minimize over non-negative arc costs, an optimal solution yields a Steiner tree. However, by introducing $b^T x \geq d$, one can add arcs (increasing the values of x) to the solution until the “ \geq ” condition holds without violating the Steiner cut constraint (5). These arcs, however, do not necessarily have to be connected to the root component. To avoid this problem, instead of considering which potential terminals are taken into account, we are interested in which

potential terminals are not considered, i.e., which newly-added terminal is directly connected to the root r by the newly-added arc (r, t'_i) and not via the original potential terminal. Thus, to fulfill the quota, there is an upper limit on how many newly-added terminals are connected directly to the root r ; see (11).

Now, let A_r denote the set of arcs from the root node r to the newly-added fixed terminals T'_f and A_t the set of arcs from the original potential terminals T_p to the newly-added fixed terminals T'_f . Let $A' = A \cup A_r \cup A_t$. Formulated as an IP, the problem reads as follows:

$$\min \quad c^T x \tag{9}$$

s.t.

$$x(\delta^-(W)) \geq 1 \quad \forall W \subset V', r \notin W, |W \cap T'| \geq 1 \tag{10}$$

$$\sum_{i' \in T'_f} q_{i'} x_{r,i'} \leq \sum_{i' \in T'_f} q_{i'} - Q \tag{11}$$

$$x_{ij} \in \{0, 1\} \quad \forall (i, j) \in A' \tag{12}$$

Let $I_{\text{QT}} = (V', A', T', c', q', Q)$ denote an instance of the transformed QSTP. Figure 1 shows the original graph and its transformation.

2.1.2 Equivalence of the LP-relaxations

We show the equivalence of the LP-relaxations of the I_Q and the I_{QT} , which are denoted by LP_{I_Q} and $LP_{I_{\text{QT}}}$, respectively. Let $v(P)$ denote the value of the optimal solution of a mathematical programming formulation P and let $\mathcal{P}_{LP}(P)$ denote the set of feasible points of its LP relaxation. Before we compare the two LP-relaxations, let us introduce an additional set of variables in the transformed instance. For each vertex v_i from the original set of potential terminals T_p , let y'_i be defined as:

$$y'_i := x(\delta^-(v_i)). \tag{13}$$

Let this extended formulation be denoted as $\overline{I_{\text{QT}}} = (V', A', T', c', p')$. By construction this new variable does not change the solution of the transformed instance I_{QT} . However, we can now formulate the result of this section:

Proposition 2.2. *Let I_Q be an instance of the QSTP and $\overline{I_{\text{QT}}}$ its transformed problem with the additional set of variables. It holds that:*

$$\text{proj}_{xy}(\mathcal{P}_{LP}(\overline{I_{\text{QT}}})) = \mathcal{P}_{LP}(I_Q). \tag{14}$$

Proof. 1) $\text{proj}_{xy}(\mathcal{P}_{LP}(\overline{I_{\text{QT}}})) \subseteq \mathcal{P}_{LP}(I_Q)$: let (x, x^t, x^r, y') $\in \mathcal{P}_{LP}(\overline{I_{\text{QT}}})$, where x , x^t , and x^r represent the variables for the arcs in A , A_r , and A_t , respectively. It is easy to see that x satisfies constraint (5) as this must hold for every original terminal $t \in T_f$ in $LP_{I_{\text{QT}}}$, too. Now we show that x^t satisfies constraints (6) and (7).

(I) x^t satisfies (6): for each $i' \in T'_f$, the Steiner cut of the set $W' = \{v_{i'}\}$ yields:

$$x(\delta^-(v_{i'})) = x_{ri'} + x_{ii'} \geq 1 \quad \Leftrightarrow \quad x_{ri'} \geq 1 - x_{ii'} \tag{15}$$

Then, for each $i' \in T'_f$ and for every W' with $\{v_i, v_{i'}\} \subseteq W'$, the Steiner cut yields:

$$x(\delta^-(W')) = x_{ri'} + x(\delta^-(W' \setminus v_{i'})) \geq 1 \tag{16}$$

Note that by construction there solely exists an arc (i, i') and no arc (i', i) . Using (15), (16), this gives:

$$\begin{aligned} x_{ri'} + x(\delta^-(W' \setminus v_{i'})) &\stackrel{(15)}{\geq} 1 - x_{ii'} + x(\delta^-(W' \setminus v_{i'})) \geq 1 \\ &\Leftrightarrow x(\delta^-(W' \setminus v_{i'})) \geq x_{ii'}. \end{aligned}$$

However, $W' \setminus v_{i'} = W$ with $W \subset V$ and $|W \cap T_p| \geq 1$. Thus, $x_{ii'}$ satisfies (6) for all $i \in T_p$. By definition, y_i also satisfies (6) for all $v_i \in T_p$. Moreover, let $W' = \{v_i, v_{i'}\}$ and then:

$$x_{ii'} \leq x(\delta^-(W' \setminus v_{i'})) = x(\delta^-(v_i)) = y_i' \quad (17)$$

(II) x^t and y satisfy (7): given constraint (11)

$$\begin{aligned} \sum_{i' \in T_f'} q_{i'} - Q &\geq \sum_{i' \in T_f'} q_{i'} x_{ri'} \stackrel{(15)}{\geq} \sum_{i' \in T_f'} q_{i'} (1 - x_{ii'}) \\ &\Leftrightarrow -Q \geq - \sum_{i' \in T_f'} q_{i'} x_{ii'} \\ &\Leftrightarrow Q \leq \sum_{i' \in T_f'} q_{i'} x_{ii'} \stackrel{(17)}{\leq} \sum_{i \in T_p} q_i y_i'. \end{aligned}$$

Hence, x^t and y satisfy (7). Finally, by ignoring x^r , we have $proj_{xy}(\mathcal{P}_{LP}(\overline{I_{QT}})) \subseteq \mathcal{P}_{LP}(I_Q)$.

2) $proj_{xy}(\mathcal{P}_{LP}(\overline{I_{QT}})) \supseteq \mathcal{P}_{LP}(I_Q)$:

Let $(\hat{x}, \hat{y}) \in \mathcal{P}_{LP}(I_Q)$. Construct (x, x^t, x^r, y) . For all $(i, j) \in A$, set $x_{ij} = \hat{x}_{ij}$. For all $i \in T_p$, set $x_{ii'}^t = y_i = \hat{y}_i$. Using (15), choose $x_{ri'} \geq 1 - \hat{y}_i$ for all $(r, i') \in A_r$. Reversing the steps of the first part of the proof, we see that (x, x^t, x^r) satisfies (10)–(11) and, so, $(x, x^t, x^r, y) \in \mathcal{P}_{LP}(I_{QT})$. Hence, $proj_{xy}(\mathcal{P}_{LP}(\overline{I_{QT}})) \supseteq \mathcal{P}_{LP}(I_Q)$, which concludes the proof. \square

2.2 Bi-objective QSTP

As mentioned in the introduction, not only costs but also other social or environmental impacts must be taken into account when planning new wind farms. In this study, we focus on minimizing both costs and the impact on the landscape of network cables and wind turbines. In addition to the cable (edge) costs c and wind turbine (potential terminal) costs w introduced in Section 2, let $s(e)$ and $s^v(v)$ denote the scenic impact of an edge $e \in E$ and of a vertex $v \in T_p$, respectively. Given an undirected graph $G = (V, E)$, a set of fixed terminals $T_f \subset V$, and a set of potential terminals $T_p \subset V$ with $T_f \cap T_p = \emptyset$, the goal is to find a tree $S = (E', V') \subseteq G$ that contains all terminals T_f such that the total cost

$$C(S) = \sum_{e \in E'} c(e) + \sum_{v \in T_p \cap V'} w(v) \quad (18)$$

and total impact on the landscape

$$L(S) = \sum_{e \in E'} s(e) + \sum_{v \in T_p \cap V'} s^v(v) \quad (19)$$

is minimized and a given quota $Q \in \mathbb{R}_{>0}$ is fulfilled, i.e.:

$$Q(S) = \sum_{i \in T_p \cap V'} q_i \geq Q \quad (20)$$

We are interested in finding the Pareto optimal solutions to this problem. A solution is Pareto optimal, if there exists no other feasible solution with a lower objective value for both goals [59]. Multiple ways to approach such a multi-objective optimization problem exist; see Ehrgott et al. [59] for a general overview. In the context of STP, Leitner et al. [60] proposes an ε -constraint algorithm to solve a bi-objective PCSTP. In this study, we compose a new objective function \bar{C} by using a convex combination of the real costs c and w and the scenic impact s and s^v as follows:

$$\bar{C}(S) = \alpha C(S) + (1 - \alpha)L(S), \quad (21)$$

where $\alpha \in [0, 1]$. Depending on the choice of α , a different solution is found, with $\alpha = 1.0$ only taking costs into account and $\alpha = 0.0$ only considering the scenic impact. The advantage of this weighted sum approach is that, in contrast to other methods like the ε -constraint one, we can retain the general structure of the single-objective QSTP formulation [59].

2.3 Shortest path reduction

In general, reduction techniques reduce the size of the original problem by removing arcs and vertices without cutting the optimal solution. Reduction techniques are often used in a preprocessing step to create "easier to solve" instances.

A common and intuitive reduction test is the shortest path reduction: If there exists a directed path $P(v, w) = \{v, (v, v_1), v_1, (v_1, v_2), \dots, v_n, (v_n, w), w\}$ of costs $c(P(v, w))$ with

$$c(P(v, w)) < c(v, w)$$

then arc (v, w) can be removed.

Proposition 2.3. *Consider an instance $I_{QT} = (V', A', T', c', q', Q)$ of the previously-described QSTP. If there exists a directed path $P(v, w)$ with costs $c(P(v, w)) < c(v, w)$, then there also exists a directed path $P(w, v)$ with costs $c(P(w, v)) < c(w, v)$, and both (v, w) and (w, v) can be removed from I_{QT} .*

Proof. Given the path $P(v, w)$ with

$$c(P(v, w)) < c(v, w)$$

each node $v_i \in \{v, v_1, \dots, v_n, w\}$ on the path $P(v, w)$ is either in T_p , i.e., $w_{v_i} > 0$, or not, i.e., $w_{v_i} = 0$. Now, subtracting the costs of node w , w_w , and adding the costs of node v , w_v , yields:

$$\begin{aligned} c(P(v, w)) - w_w + w_v &< c(v, w) - w_w + w_v \\ c(v, v_1) + c(v_1, v_2) + \dots + c(v_n, w) - w_w + w_v &< c(v, w) - w_w + w_v \end{aligned} \quad (22)$$

The cost of an arc (i, j) is given by $c(i, j) = c_e + w_j$ where c_e is the costs of the undirected edge $e = (i, j)$. With this, (22) reads as follows:

$$\begin{aligned} \underbrace{c(v, v_1)}_{c(v, v_1)} + w_{v_1} + \underbrace{c(v_1, v_2)}_{c(v_1, v_2)} + w_{v_2} + \dots + \underbrace{c(v_n, w)}_{c(w, v_n)} + w_w - w_w + w_v &< c_{v, w} + w_w - w_w + w_v \\ w_v + \underbrace{c_{v, v_1}}_{c(v, v_1)} + \underbrace{w_{v_1} + c_{v_1, v_2}}_{c(v_1, v_2)} + \dots + \underbrace{w_{v_n} + c_{v_n, w}}_{c(w, v_n)} &< c_{v, w} + w_v \\ c(P(w, v)) &< c(w, v) \end{aligned}$$

Hence, a path $P(w, v)$ with costs less than the those of arc (w, v) also exists. \square

2.4 Shortest path heuristic

Heuristics are used to find good and feasible solutions in short time, and thus providing upper bounds on the exact solution of a problem. In the context of STP, one of the best-known heuristics is the *shortest path heuristic*, which was introduced by Takahashi & Matsuyama [61]. For this study, we adapt the implementation of the shortest path heuristic given by Rehfeldt [62]. Starting at the root node, we add the closest fixed terminal or potential terminal to the root component. Then we update the distance of all non-connected vertices to the root component. We repeat until all fixed terminals are connected and the connected potential terminals fulfill the desired quota.

3 Computational results

In this section, we describe the input data, the computational setup, and the computational results. The QSTP ((4) – (8)) and its transformation ((9) – (12)) are integrated in the general STP solver SCIP-JACK. SCIP-JACK uses a branch-and-cut procedure to account for the exponential number of constraints induced by the Steiner cut-like constraints, i.e., (5), (6), and (10). We use the native, flow-based separation algorithm of SCIP-JACK for the Steiner-cut generation and add the additional quota constraint. Most other features of SCIP-JACK, such as heuristics, reduction methods, and domain propagation, do not work with the quota constraints and must be turned off. Therefore, we implemented the shortest-path-based reduction method, which is used in the presolving step. As to primal heuristics, we implement the shortest-path heuristic as primal heuristic, to improve the solving process. The heuristic might find an optimal solution or gives a primal bound, with which nodes of the branch-and-bound tree can be removed. Depending on the current LP-solution the shortest-path heuristic is called repeatedly on a graph with modified arc costs $\bar{c}_a = (1.0 - \hat{x})_{c_a}$ for all $a \in A$ during the branch-and-bound procedure.

3.1 Input data, case studies and computations

The considered wind turbines are potential turbines with costs and designs for the year 2050 from Ryberg et al. [63]. To determine their locations, state-of-the-art methods were applied to exclude unsuitable areas, for example due to high terrain steepness or minimal distances to settlements or infrastructure. Ryberg et al. [63] obtained the costs for the wind turbines as well as their annual energy yields. The specific costs for cables and the grid connection of turbines are based on McKenna et al. [32]. The data for substation locations is based on OpenStreetMap [64] entries.

The scenic features of landscapes in Germany are derived from Roth et al. [65], who for the first time conducted an area-wide analysis of the aesthetic value of landscapes across the country. Using selected photographs, a survey and subsequent regression, each 1 km² in Germany was assigned an aesthetic value from one (low scenic quality) to nine (high scenic quality) (see Figure 2). For the showcase of our methodology, we assume that one km of electricity network has the same impact on the landscape as one wind turbine.

In the following, we apply the previously described models to two case study regions in Germany (see Figure 2). The first of these, case study A, includes the siting and grid connection planning of potential wind turbines in the municipalities of Bad Bellingen and Schliengen. In these two municipalities, a total of 22 potential turbines can be connected to three different substations with a total annual energy yield of 158 GWh. A choice can be made between 122 Steiner points and 10,731 possible edges. In case study B, the optimization problem was applied to a much larger German region with 65 possible turbines with a total energy yield of 405 GWh, with eight substations, 1566 Steiner points and 1.35 million edges. The Steiner points were placed in a grid with the dimensions of 1000 meters (case study A) and 500 meters (case study B) using the geographic information system QGIS. Then, a PYTHON script was developed to determine all possible interconnecting edges. This script can be automatically applied to any given region and can be provided upon request.

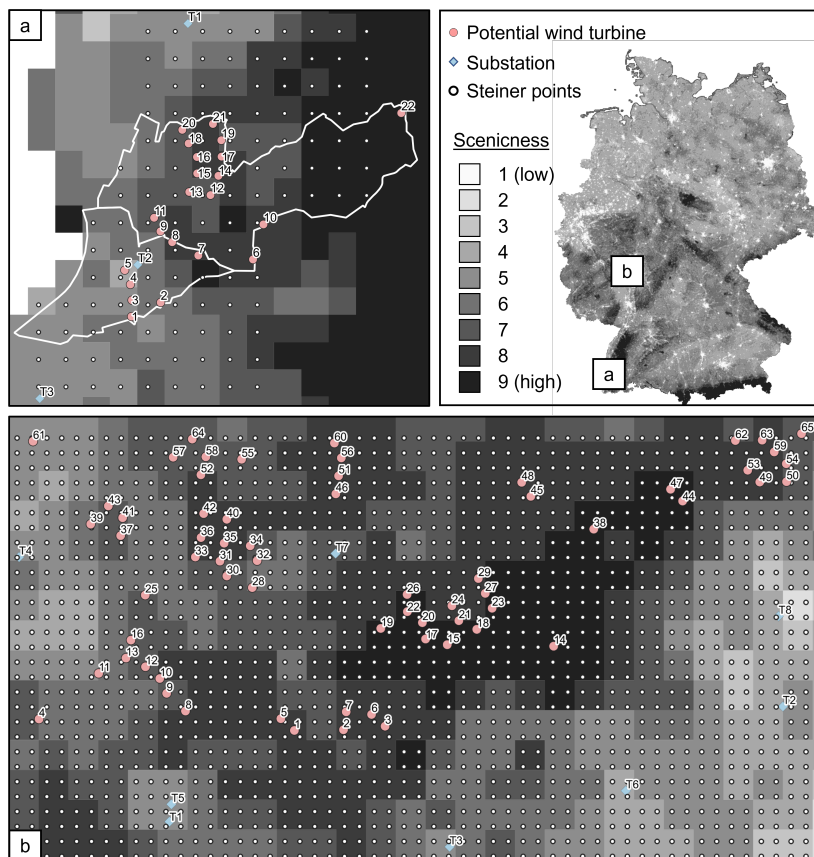


Figure 2: Substations, potential wind turbines, Steiner points, and scenic value in case studies A and B in Germany. The map of Germany shows the locations of the two case studies as well as the landscape’s scenic value distribution in Germany.

For each of the two case study regions, we generate a set of instances on which we evaluate our proposed techniques. We vary both the given quota Q and weight of the cable costs and scenic value α , resulting in different edge costs. For region A, we choose the following quotas $Q \in [10, 20, 30, 40, 50, 60, 70, 80, 90, 100, 110, 120, 130, 140, 150, 158]$ and for region B we choose $Q \in [50, 100, 150, 175, 200, 250, 300, 350, 405]$. For both regions, we let α increase from 0.0 to 1.0 in 0.1 steps. This results in 176 instances for region A and 99 for region B. The substations are modeled as fixed terminals T_f . To allow subtrees, all substations are interconnected by edges of zero costs. The wind turbines are modeled as potential terminals T_p .

We verify our proposed formulation by solving the problem with the general out-of-the-box MIP solver GUROBI [66]. Due to the exponential number of constraints given by (10), we model the problem as the following flow-based MIP formulation (FLOW). Let $r \in T_f$ be chosen as root. Note that in our case as all substations (terminals) are interconnected by edges of zero costs, it does not matter which terminal is chosen as the root. The flow-based MIP formulation is given by

$$\min \quad c^T x + w^T y \quad (23)$$

$$\text{s.t.} \quad (24)$$

$$\sum_{v \in T_p} q_v y_v \geq Q \quad (25)$$

$$\sum_{a \in \delta^-(v)} f_a - \sum_{a \in \delta^+(v)} f_a = \begin{cases} 0 & \forall v \in V \setminus (T_f \cup T_p) \\ 1 & \forall v \in T_f \setminus r \\ y_v & \forall v \in T_p \end{cases} \quad (26)$$

$$x_a \leq y_v \quad \forall a \in \delta^-(v), \forall v \in T_p \quad (27)$$

$$f_a \leq M x_a \quad \forall a \in A \quad (28)$$

$$y_v \in \{0, 1\} \quad \forall v \in T_p \quad (29)$$

$$x_a \in \{0, 1\}, f_a \in \mathbb{R}_{\geq 0} \quad \forall a \in A \quad (30)$$

where x and y denote the decision variables if an arc and a vertex is chosen, respectively, and f describes the flow over the arcs. Constraint (25) describes the quota constraint and (26) captures the flow balance at each vertex depending on its type. The incoming arcs of a potential terminal can only be active if the potential terminal is chosen, as in (27). Equation (28) ensures that a flow over an arc is only possible if the arc is active. We choose $M = |T_p|$ as an upper limit for the maximum capacity of the arcs. The flow-based formulation was implemented in PYTHON 3.8.10 using the GUROBI PYTHON-interface, and is solved with GUROBI 9.5 [66]. For the QSTP and its transformation we use SCIP-JACK in SCIP 8.0.1 [67] using CPLEX 12.10 [68] as the LP solver.

We solve the instance sets described above with the following settings: a) the flow-based formulation (FLOW with GUROBI), b) the initial QSTP formulation QSTP, c) the transformed QSTP TransQSTP, d) the transformed QSTP plus a shortest-path reduction TransQSTP+, and e) the transformed QSTP plus the shortest-path reduction and plus a shortest-path based heuristic TransQSTP++. All computations were executed single-threaded in the case of SCIP-JACK and with 32 threads in the case of GUROBI on a cluster with *Intel XeonGold 6342* CPUs running at 2.8 GHz and with 30 GB of RAM. We set a time limit of six hours (21,600 s).

3.2 Comparison with state-of-the-art generic solvers

The summary of the computational results is presented in Table 1 and Table 2 (for the detailed results see Table A.1 and A.2 in the appendix) for the instances of region A and region B, respectively.

In the case of region A, all 176 instances were solved to optimality within the time limit of 3600s with all approaches. However, there was a significant difference in the time needed to solve the instances. As expected, the naive flow formulation solved by the standard out-of-the-box MIP solver was significantly outperformed by an order of magnitude for the QSTP and by two orders of magnitude for the TransQSTP++ (see Figure 3a). Almost 80% of the instances were solved in less than one second for TransQSTP++ and TransQSTP, TransQSTP+ as well as TransQSTP++, which solved all the instances in less than ten seconds. On the other hand, QSTP needs ten seconds to solve 60% and 100 seconds to solve all instances. With the out-of-the-box MIP solver, less than 50% of the instances were solved after 100 seconds. To solve all instances, the MIP solver needs 3000 seconds on the instance set of region A.

Following the results for region A, we excluded the flow and the original QSTP formulation when solving the instances of region B (see Table 2). TransQSTP only finds an optimal solution for a single instance in over 11000 seconds and solutions for six additional instances, with an average optimality gap of $> 600\%$. As is shown in the performance profiles in Figure 3b, TransQSTP++ reaches 80% of the solved instances within around 16,500 seconds, but does not manage to solve the remaining 20 instances to optimality within the time limit of six hours. However, TransQSTP++ provides solutions for the missing instances with an average gap of

1.2% and a maximum gap of $< 15\%$. **TransQSTP+** solves 60 out of 99 instances to optimality and provides solutions for 13 more instances with an average gap of 16% and maximum gap of around 300% within the time limit.

Table 1: Summary of computational results for region A.

Name	# Instances	# Solved	# Optimal	\varnothing Time [s]
TransQSTP + Heuristic + Reduction	176	176	176	0.86
TransQSTP + Reduction	176	176	176	1.58
TransQSTP	176	176	176	3.31
QSTP	176	176	176	10.24
Flow with GUROBI	176	176	176	378.09

Table 2: Summary of computational results for region B. The gap is averaged over all instances with a non-optimal solution; the time is averaged over all instances, which are solved to optimality.

Name	# Instances	# Solved	# Optimal	\varnothing Gap [%]	\varnothing Time [s]
TransQSTP++	99	99	79	1.2	4039.23
TransQSTP+	99	83	60	16.0	6977.53
TransQSTP	99	7	1	666.0	11552.30

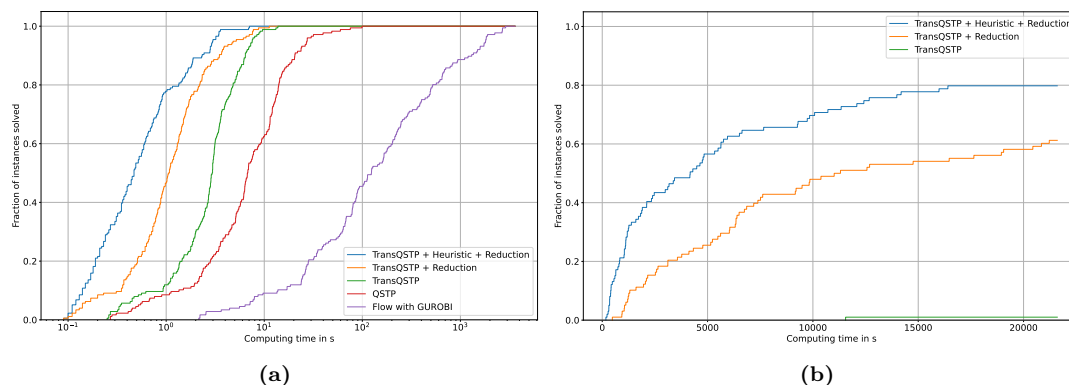


Figure 3: Performance profiles for region A (Panel 3a) and B (Panel 3b), showing the cumulative percentage of instances solved to optimality over time for all approaches. The Computing time in 3a is shown on a log-scale

Figure 4 shows the computing time of **TransQSTP++** for each instance. In general, higher α , i.e., less weight of scenic impact, led to a higher run time. This is due to the fact that the shortest path reduction is not effective if only costs are considered, as the direct connection between nodes is also the shortest one. However, decreasing α (see gray scaling in Figure 4) leads to a higher influence of the scenic value, with more edges deleted, and, so the problem size becomes smaller. The solution time increases with a higher share of the desired quota until 300.0 (around 75% of maximal quota) is reached. With an increasing quota share, there is a higher flexibility in placing turbines and cables with similar costs (scenic value), making it more difficult to find the optimal solution. The choice of turbines becomes more limited with very high quota shares as up to all turbines must be built, leaving only the cable routing as flexibility, resulting in decreasing computing times (compared to the peak at around 75% of quota share). Even though our approach finds solutions for quota shares of 100%, the QSTP reduces to the general STP problem by considering all turbines (potential terminals) as fixed terminals in this case (see Observation 2.1), which can be solved much faster with SCIP-JACK.

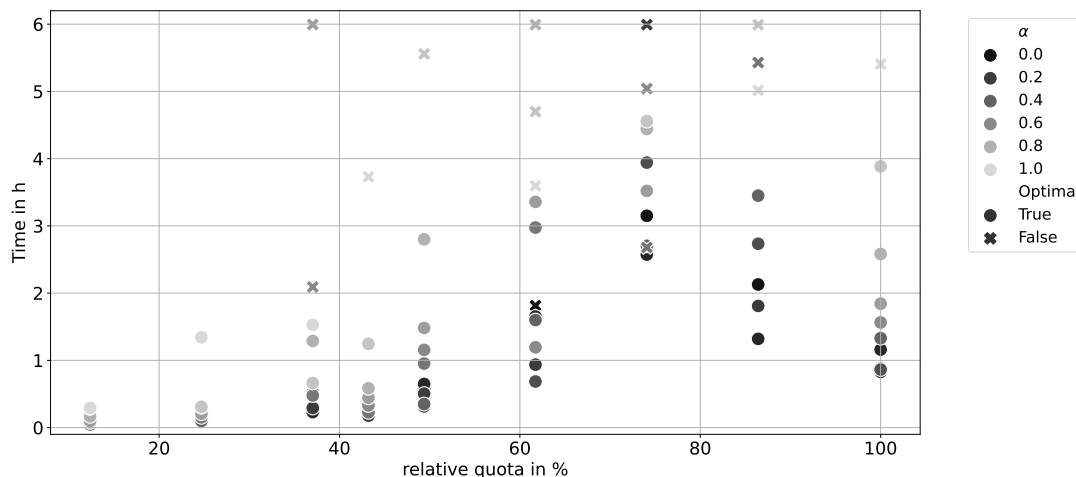


Figure 4: Solution time for instances of region B solved by **TransQSTP++** for each quota. The quota is shown relative to the maximal possible potential. The gray scale represents the weight α between the costs and the scenic impact. The cross markers indicate instances that have not been solved to proven optimality.

3.3 Trade-offs between costs and scenic value

The trade-offs between cost and scenic value depend to a large extent on the conditions of the region as well as on the quota, i.e. how much of the maximum possible electricity supply by wind turbines is required (see Figures 5 and 6). For low quotas, the solution space offers little flexibility: region A has only one solution for any given α for quotas of 10 and 20 GWh (Figure 5d), and region B has only two solutions for the lowest quotas of 50 and 100 GWh (Figure 6e). Thus, for the latter problems, no trade-off between cost and scenic value is possible. Either the decision is made to minimize cost while increasing scenic impact by 8% (quota of 50 GWh) or 5% (100 GWh), or the focus is on scenic value while increasing costs by 4% (50 GWh) or 8% (100 GWh). Likewise, the planning flexibility is low at very high quotas, as in these cases the wind turbines are more or less fixed and the costs and landscape impacts can only be influenced by the connection of the turbines to the substations.

In contrast to the previous insights, planning flexibility is somewhat high for medium quotas. For example, in region A, for a quota of 40 GWh, scenic value can be reduced by almost 20% or costs by 14% (Figure 5d). A similar trend can be observed for a quota of 70 GWh; for this, Figure 5a-5c shows how turbine selection and power networks would vary depending on the weighting of costs and scenic value. The Pareto curves are particularly interesting, however, for the larger region B, such as at quotas of 250 or 300 GWh: in these cases, costs can be reduced by about 5% with almost unchanged landscape impact (Figure 6e). The larger the region and so the more turbines or substations can be chosen, the more our approach can assist in finding Pareto-optimal solutions for local residents or wind farm operators.

3.4 Large-scale siting must include grid integration

Planning wind turbine expansion on a national level leads to suboptimal solutions in terms of cost and landscape impact if grid integration is neglected. We demonstrate this by comparing our approach with the scenarios from Weinand et al. [27], who identified the optimal turbine locations at the national level for Germany assuming a capacity of 200 GW in the year 2050 (Figure 7). In Weinand et al. [27], only the costs and scenic value of the turbine sites were taken into account, but not for the networks, as a simultaneous optimization of both factors was hardly computationally practicable for such a large region. In order to comparatively assess the turbine locations in Weinand et al. [27] using our approach, we first connected the

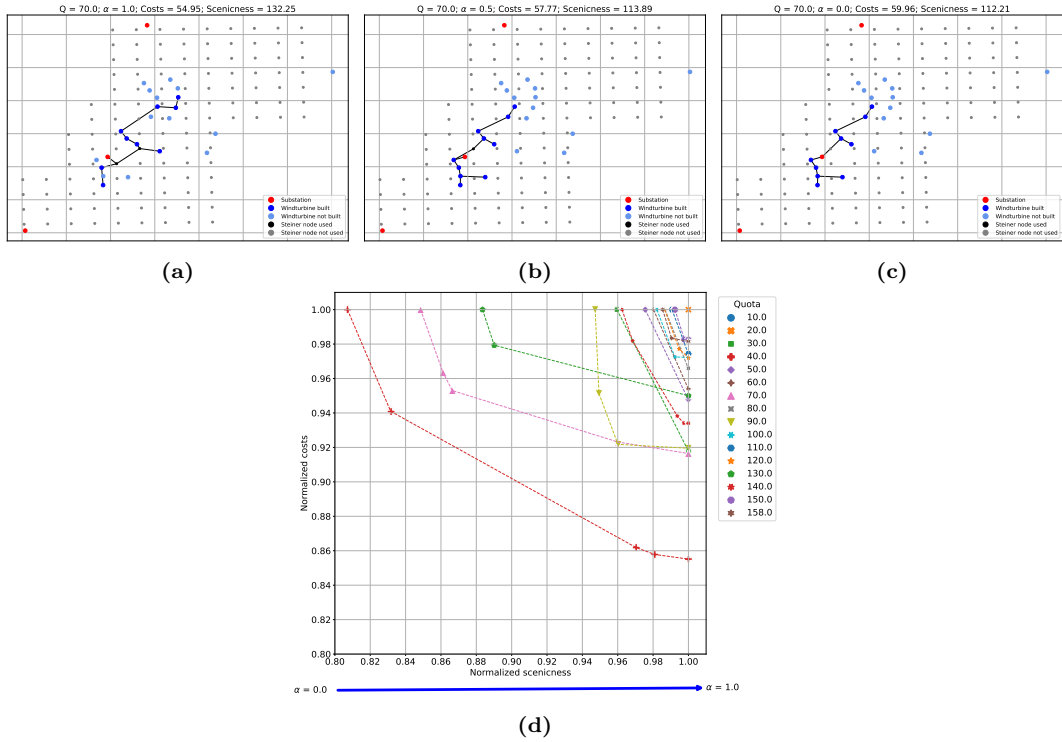


Figure 5: Solution for different α values with a quota of $Q = 70.0$ of region A (Panels 5a-5c). Panel 5d shows normalized scenic value versus normalized costs for each quota in region A. The normalization was performed for each curve by dividing the values by the respective maximum cost or scenic value value for the corresponding quota. This means that the curves for different quotas are not comparable to each other, but for each quota the trade-offs between scenic value and cost are shown.

turbines from Weinand et al. [27] to the substations while minimizing costs or scenic value. This is consistent with the methodology developed in this study, but with turbine sites fixed in advance. When minimizing costs, selecting turbine sites without simultaneously considering network costs can result in 21% higher total costs than simultaneously optimizing sites and network connection costs (Figure 7a and Figure 7b). The same is true for the landscape impact, which is 39% lower with the simultaneous optimization of turbines and networks (Figure 7c & Figure 7d). Interestingly, the shorter network cables chosen in our novel approach would always also lead to lower values for the criterion that was not been chosen as the objective. For example, if scenic value were to be minimized for a quota of $Q = 137$ GWh (as for the cost minimizations in Figure 7a & Figure 7b), the overall costs would still be 10% lower than for the approach with fixed turbine siting and subsequent cost-optimized network connections.

In the future, it is essential that recent approaches in the articles by Weinand et al. [27], Lehmann et al. [28], Tafarte & Lehmann [29], and Spielhofer et al. [69] on the optimal siting of turbines on a national level attempt to simultaneously include the network integration. For this purpose, approaches should be developed to make the methodology used in this study applicable to very large regions, such as entire countries.

4 Discussion and conclusions

Current methods for planning onshore wind farms and integrating them into networks do not always meet minimum cost solutions or account for social and environmental factors. This paper proposes a new approach for optimizing turbine locations and network connections using a Quota Steiner tree problem (QSTP). We present a novel transformation of the already known directed cut formulation of the QSTP. Even though the LP-relaxations of the transformed and

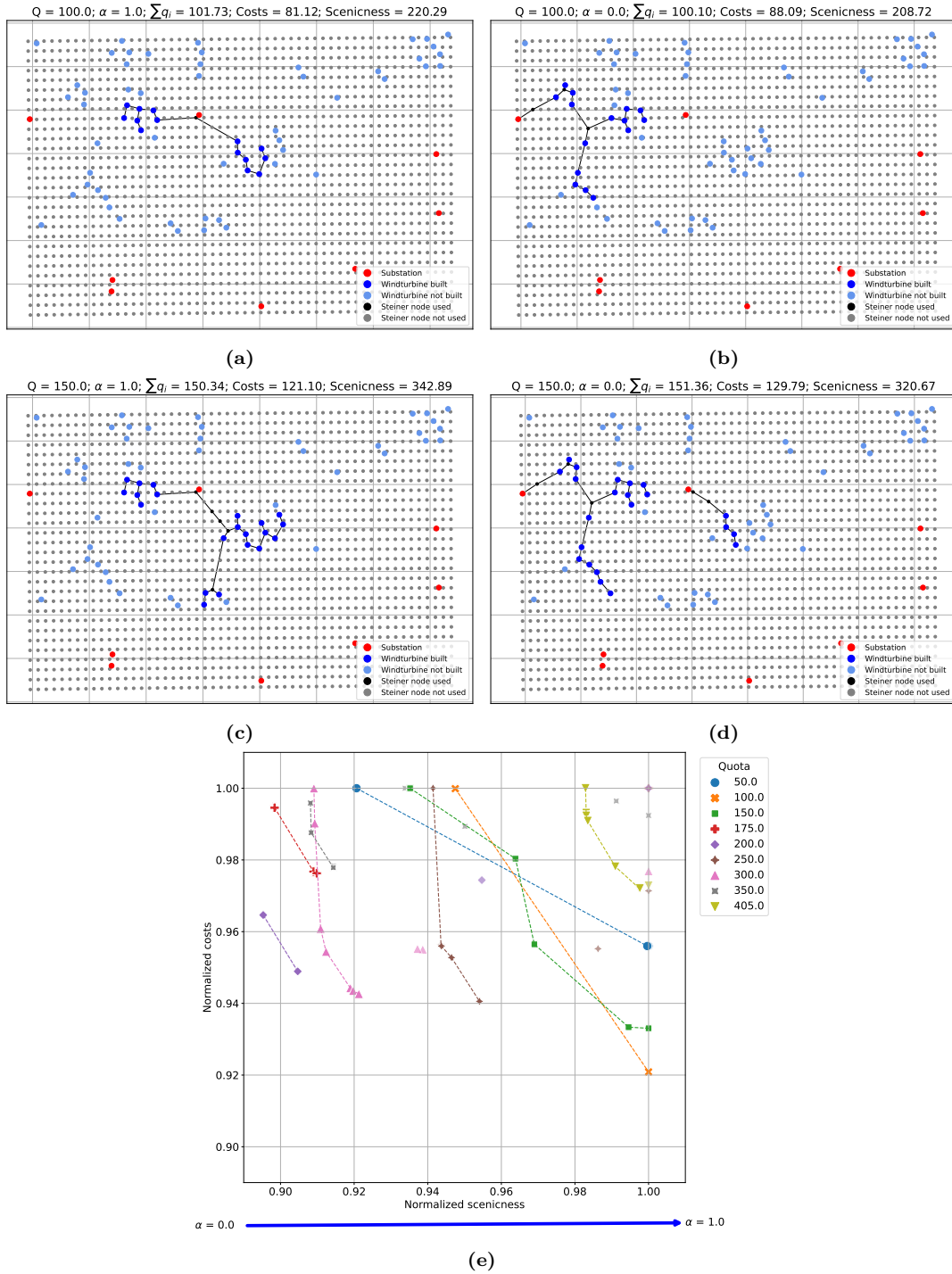


Figure 6: Solution for a quota of $Q = 100.0$ with $\alpha = 1.0$ (Panel 6a) and $\alpha = 0.0$ (6b) and for a quota of $Q = 150.0$ with $\alpha = 1.0$ (6c) and $\alpha = 0.0$ (6d) of region B. Panel 6e shows normalized scenic value versus normalized costs for each quota in region B. The normalization was performed for each curve by dividing the values by the respective maximum cost or scenic value for the corresponding quota. This means that the curves for different quotas are not comparable to each other, but for each quota the trade-offs between scenic value and cost are shown. Transparent points are not Pareto optimal, as these are solutions with an optimal gap $> 0\%$.

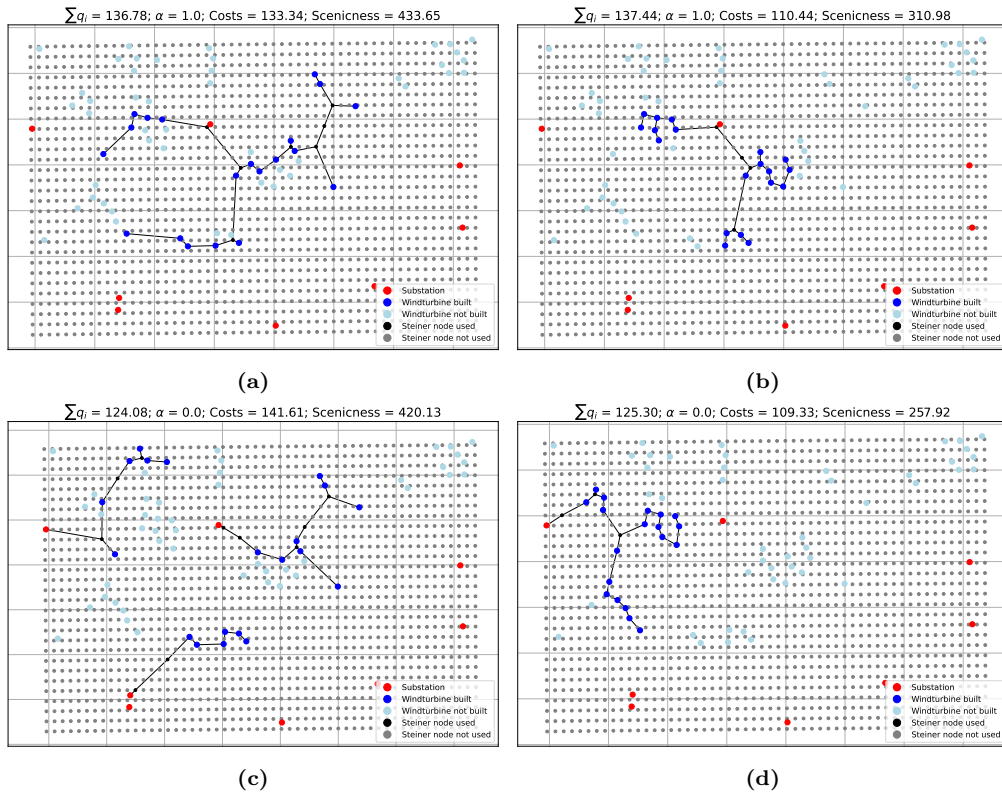


Figure 7: Solution for minimizing the costs ($\alpha = 1.0$) with a quota of around $Q = 137.0$ in region B (a and b), and for minimizing the scenic value ($\alpha = 0.0$) with a quota of around $Q = 124.0$ in region B (c and d). TPanels a and c show the optimal turbine locations at the state level for Germany assuming a capacity of 200 GW in 2050 from [27], which did not involve simultaneous network planning. Based on the fixed turbine locations, we used our optimization model to connect these turbines to substations. Panels b and d represent the optimal solutions based on our approach with simultaneous turbine and network optimization.

original formulation are proven to be equivalent, the transformed formulation proves to be more effective in practice. By using shortest path reduction and the shortest path heuristic, we have advanced the state-of-the-art STP-solver SCIP-JACK in the context of QSTP, which outperforms standard solvers and is capable of solving large-scale problems with up to at least 1.3 million edges. Our case studies, conducted in selected regions of Germany, demonstrate significant trade-offs between cost and landscape impacts when planning onshore wind farms. However, we also show that small reductions in one objective criterion can yield significant improvements in the other. Additionally, we illustrate that simultaneously optimizing network integration with turbine siting is essential for avoiding excessive costs or landscape impacts in the course of wind farm projects.

In this study, our focus was on presenting the applicability and utility of the methodology. For real case studies, further important criteria beyond costs and landscape impacts should be considered in the future. For example, disamenities for the local population should be incorporated [28–30], as well as the environmental impacts of turbines, e.g., through bird strikes [70] and land use competition with other renewable energy sources [71]. Furthermore, we used different weightings in our multi-objective planning without knowing the exact preferred weightings between the two objectives costs and scenic value. In addition, equating the landscape impact of a wind turbine with that of a 1 km electricity network is a strong simplification. However, previous research has demonstrated that finding universally valid weights between target criteria in wind farm planning is nearly impossible, even for experts [72]. In regional planning, such as that discussed in this paper, local stakeholders could be consulted in multi-criteria decision approaches to determine appropriate weightings in the future [73].

Furthermore, we select the Steiner points independently of the geographical conditions. Our problem could be improved by using a digital elevation model to determine true distances and by taking obstacles into account for which the cables cannot be deployed (see also Fischetti & Pisinger [40]). In addition, for larger regions, we were not able to find solutions for all instances. Especially when transferring our methodology to federal states or countries, further methodological advancements will be necessary to make this computable. For example, reduction techniques are one of the most essential and effective features in solving STP-related problems [44] and SCIP-JACK provides many strong reduction techniques, see e.g., [62, 74, 75]. Therefore, identifying efficient reduction techniques could significantly improve the solution process, however, these have yet to be studied in the context of QSTPs. When investigating larger regions and wind farms, future studies should also incorporate the meshing of power grids for increased security of supply as well as the (remaining) capacities of substations. The existing substations we have considered may not always have sufficient remaining capacity to ensure the grid connection of further wind farms and new substations would have to be installed. Additionally, we used a shortest path heuristic to find primal solutions in the branch-and-cut algorithm. In the future, developing new primal and dual heuristics in the context of QSTP could be a promising way to further improve our approach. For instance, exploration of the idea of Leitner et al. [54] who introduced a dual-ascent algorithm in the context of PCSTPs could be worthwhile. Although our approach is also applicable for planning other renewable energy plants like solar photovoltaic installations, applications of the algorithm beyond energy system analysis are also conceivable: for example, cable routing optimization approaches for offshore wind farms [40, 41] were recently applied to determine safe distancing during the COVID-19 pandemic [76].

Acknowledgements

The work for this article has been conducted in the Research Campus MODAL funded by the German Federal Ministry of Education and Research (BMBF) (fund numbers 05M14ZAM, 05M20ZBM). Furthermore, this work was supported by the Helmholtz Association under the program "Energy System Design".

CRediT statement

Conceptualization: J.W., J.P., D.R.; data curation: J.W., C.S., J.P.; formal analysis: J.P., J.W.; investigation: J.P., J.W.; methodology: J.P., D.R., J.W.; software: J.P., D.R.; validation: J.P., J.W.; visualization: J.P., J.W.; writing – original draft: J.P., J.W.; writing – review and editing: J.P., J.W., D.R.

References

1. Veers, P., Dykes, K., Lantz, E., Barth, S., Bottasso, C. L., Carlson, O., Clifton, A., Green, J., Green, P., Holttinen, H., Laird, D., Lehtomäki, V., Lundquist, J. K., Manwell, J., Marquis, M., Meneveau, C., Moriarty, P., Munduate, X., Muskulus, M., Naughton, J., Pao, L., Paquette, J., Peinke, J., Robertson, A., Sanz Rodrigo, J., Sempreviva, A. M., Smith, J. C., Tuohy, A. & Wisler, R. Grand challenges in the science of wind energy. *Science (New York, N.Y.)* **366** (2019).
2. Pryor, S. C., Barthelmie, R. J., Bukovsky, M. S., Leung, L. R. & Sakaguchi, K. Climate change impacts on wind power generation. *Nature Reviews Earth & Environment* **1**, 627–643 (2020).
3. Our World in Data. *Installed wind energy capacity 2021*. <https://ourworldindata.org/grapher/cumulative-installed-wind-energy-capacity-gigawatts?country=ESP~IND~AUS~DEU~JPN~ITA~CHN> (Accessed on 08/21/2021).
4. Wisler, R., Jenni, K., Seel, J., Baker, E., Hand, M., Lantz, E. & Smith, A. Expert elicitation survey on future wind energy costs. *Nature Energy* **1** (2016).
5. Wisler, R., Rand, J., Seel, J., Beiter, P., Baker, E., Lantz, E. & Gilman, P. Expert elicitation survey predicts 37% to 49% declines in wind energy costs by 2050. *Nature Energy* **6**, 555–565 (2021).
6. Jansen, M., Staffell, I., Kitzing, L., Quoilin, S., Wiggelinkhuizen, E., Bulder, B., Riepin, I. & Müsgens, F. Offshore wind competitiveness in mature markets without subsidy. *Nature Energy* **5**, 614–622 (2020).
7. IEA. *Renewables 2020: Analysis and forecast to 2025. Wind*. 2021. <https://www.iea.org/reports/renewables-2020/wind> (Accessed on 02/26/2021).
8. Reusswig, F., Braun, F., Heger, I., Ludewig, T., Eichenauer, E. & Lass, W. Against the wind: Local opposition to the German Energiewende. *Utilities Policy* **41**, 214–227. ISSN: 09571787 (2016).
9. Rand, J. & Hoen, B. Thirty years of North American wind energy acceptance research: What have we learned? *Energy Research & Social Science* **29**, 135–148. ISSN: 22146296 (2017).
10. Weinand, J. M., McKenna, R., Kleinebrahm, M., Scheller, F. & Fichtner, W. The impact of public acceptance on cost efficiency and environmental sustainability in decentralized energy systems. *Patterns (New York, N.Y.)* **2**, 100301 (2021).
11. Fast, S., Mabee, W., Baxter, J., Christidis, T., Driver, L., Hill, S., McMurtry, J. J. & Tomkow, M. Lessons learned from Ontario wind energy disputes. *Nature Energy* **1** (2016).
12. Boudet, H. S. Public perceptions of and responses to new energy technologies. *Nature Energy* **4**, 446–455 (2019).
13. Petrova, M. A. From NIMBY to acceptance: Toward a novel framework — VESPA — For organizing and interpreting community concerns. *Renewable Energy* **86**, 1280–1294. ISSN: 09601481 (2016).
14. Suškevičs, M., Eiter, S., Martinat, S., Stober, D., Vollmer, E., de Boer, C. L. & Buchecker, M. Regional variation in public acceptance of wind energy development in Europe: What are the roles of planning procedures and participation? *Land Use Policy* **81**, 311–323. ISSN: 02648377 (2019).

15. Wolsink, M. Co-production in distributed generation: renewable energy and creating space for fitting infrastructure within landscapes. *Landscape Research* **43**, 542–561. ISSN: 0142-6397 (2018).
16. Molnarova, K., Sklenicka, P., Stiborek, J., Svobodova, K., Salek, M. & Brabec, E. Visual preferences for wind turbines: Location, numbers and respondent characteristics. *Applied Energy* **92**, 269–278. ISSN: 03062619 (2012).
17. Spielhofer, R., Hunziker, M., Kienast, F., Wissen Hayek, U. & Grêt-Regamey, A. Does rated visual landscape quality match visual features? An analysis for renewable energy landscapes. *Landscape and Urban Planning* **209**, 104000. ISSN: 01692046 (2021).
18. Statista. *Global onshore wind energy capacity in 2019, by country* 2020. <https://www.statista.com/statistics/476318/global-capacity-of-onshore-wind-energy-in-select-countries/> (Accessed on 02/26/2021).
19. Clean Energy Wire. *German onshore wind power – output, business and perspectives* 2023. <https://www.cleanenergywire.org/factsheets/german-onshore-wind-power-output-business-and-perspectives> (Accessed on 03/23/2023).
20. Statista. *Approximate wind energy penetration in leading wind markets in 2019, by select country* 2020. <https://www.statista.com/statistics/217804/wind-energy-penetration-by-country/> (Accessed on 02/26/2021).
21. Clean Energy Wire. *German onshore wind power – output, business and perspectives* 2021. <https://www.cleanenergywire.org/factsheets/german-onshore-wind-power-output-business-and-perspectives> (Accessed on 02/26/2021).
22. Clean Energy Wire. *Limits to growth: Resistance against wind power in Germany* 2019. <https://www.cleanenergywire.org/factsheets/fighting-windmills-when-growth-hits-resistance> (Accessed on 02/27/2021).
23. Buck, T. Germans fall out of love with wind power. *Financial Times*. <https://www.ft.com/content/d8b9b0bc-04a6-11ea-a984-fbbacad9e7dd> (Accessed on 03/04/2021) (2019).
24. Bertsch, V., Hall, M., Weinhardt, C. & Fichtner, W. Public acceptance and preferences related to renewable energy and grid expansion policy: Empirical insights for Germany. *Energy* **114**, 465–477. ISSN: 03605442 (2016).
25. Roth, M., Hildebrandt, S., Roser, F., Schwarz-von Raumer, H.-G., Borsdorff, M., Peters, W., Weingarten, E., Thylmann, M. & Bruns, E. *Entwicklung eines Bewertungsmodells zum Landschaftsbild beim Stromnetzausbau* 2021. <https://www.bfn.de/publikationen/bfn-schriften/bfn-schriften-597-entwicklung-eines-bewertungsmodells-zum> (Accessed on 05/13/2022).
26. BWE. *Netzanschlussoptimierung* 2021. <https://www.wind-energie.de/themen/netze/netzanschlussoptimierung/> (Accessed on 11/24/2021).
27. Weinand, J. M., McKenna, R., Heinrichs, H., Roth, M., Stolten, D. & Fichtner, W. Exploring the trilemma of cost-efficiency, landscape impact and regional equality in onshore wind expansion planning. *Advances in Applied Energy* **7**, 100102. ISSN: 2666-7924 (2022).
28. Lehmann, P., Reutter, F. & Tafarte, P. *Optimal siting of onshore wind turbines: Local disamenities matter* 2021. https://www.ufz.de/export/data/global/255615_DP_2021_4_Lehmannetal.pdf (Accessed on 09/29/2021).
29. Tafarte, P. & Lehmann, P. Quantifying trade-offs for the spatial allocation of onshore wind generation capacity – A case study for Germany. *Ecological Economics* **209**, 107812. ISSN: 0921-8009 (2023).
30. Weinand, J. M., Naber, E., McKenna, R., Lehmann, P., Kotzur, L. & Stolten, D. Historic drivers of onshore wind power siting and inevitable future trade-offs. *Environmental Research Letters* **17** (2022).

31. Weinand, J. M., Sörensen, K., San Segundo, P., Kleinebrahm, M. & McKenna, R. Research trends in combinatorial optimization. *International Transactions in Operational Research* **29** (2022).
32. McKenna, R., Weinand, J. M., Mulalic, I., Petrović, S., Mainzer, K., Preis, T. & Moat, H. S. Scenicness assessment of onshore wind sites with geotagged photographs and impacts on approval and cost-efficiency. *Nature Energy* (2021).
33. Wędzik, A., Siewierski, T. & Szypowski, M. A new method for simultaneous optimizing of wind farm's network layout and cable cross-sections by MILP optimization. *Applied Energy* **182**, 525–538. ISSN: 03062619 (2016).
34. Wu, Y., Zhang, S., Wang, R., Wang, Y. & Feng, X. A design methodology for wind farm layout considering cable routing and economic benefit based on genetic algorithm and GeoSteiner. *Renewable Energy* **146**, 687–698. ISSN: 09601481 (2020).
35. Herbert-Acero, J., Probst, O., Réthoré, P.-E., Larsen, G. & Castillo-Villar, K. A Review of Methodological Approaches for the Design and Optimization of Wind Farms. *Energies* **7**, 6930–7016 (2014).
36. Cazzaro, D., Fischetti, M. & Fischetti, M. Heuristic algorithms for the Wind Farm Cable Routing problem. *Applied Energy* **278**, 115617. ISSN: 03062619 (2020).
37. Cazzaro, D. & Pisinger, D. Variable neighborhood search for large offshore wind farm layout optimization. *Computers & Operations Research* **138** (2022).
38. Hertz, A., Marcotte, O., Mdimagh, A., Carreau, M. & Welt, F. Design of a wind farm collection network when several cable types are available. *Journal of the Operational Research Society* **68**, 62–73. ISSN: 0160-5682 (2017).
39. Žarković, S. D., Shayesteh, E. & Hilber, P. Onshore wind farm - Reliability centered cable routing. *Electric Power Systems Research* **196** (2017).
40. Fischetti, M. & Pisinger, D. Optimizing wind farm cable routing considering power losses. *European Journal of Operational Research* **270**, 917–930 (2018).
41. Fischetti, M. On the optimized design of next-generation wind farms. *European Journal of Operational Research* **291**, 862–870 (2021).
42. Fischetti, M. & Fischetti, M. Integrated Layout and Cable Routing in Wind Farm Optimal Design. *Management Science*. ISSN: 0025-1909 (Aug. 2022).
43. Karp, R. M. in *Complexity of Computer Computations: Proceedings of a Symposium on the Complexity of Computer Computations, Held March 20–22, 1972, at the IBM Thomas J. Watson Research Center, Yorktown Heights, New York, and Sponsored by the Office of Naval Research, Mathematics Program, IBM World Trade Corporation, and the IBM Research Mathematical Sciences Department* (eds Miller, R. E., Thatcher, J. W. & Bohlinger, J. D.) 85–103 (Springer US, Boston, MA, 1972). ISBN: 978-1-4684-2001-2.
44. Ljubić, I. Solving Steiner Trees: Recent Advances, Challenges, and Perspectives. *Networks* **77**, 177–204. ISSN: 1097-0037 (2021).
45. Leitner, M., Ljubic, I., Luipersbeck, M., Prosegger, M. & Resch, M. *New Real-world Instances for the Steiner Tree Problem in Graphs* tech. rep. (Jan. 2014).
46. Bolukbasi, G. & Kocaman, A. S. A Prize Collecting Steiner Tree Approach to Least Cost Evaluation of Grid and Off-Grid Electrification Systems. *Energy* **160**, 536–543. ISSN: 0360-5442 (Oct. 2018).
47. Ljubić, I., Weiskircher, R., Pfersch, U., Klau, G. W., Mutzel, P. & Fischetti, M. An Algorithmic Framework for the Exact Solution of the Prize-Collecting Steiner Tree Problem. *Mathematical Programming* **105**, 427–449. ISSN: 1436-4646 (Feb. 2006).
48. Klimm, F., Toledo, E. M., Monfeuga, T., Zhang, F., Deane, C. M. & Reinert, G. Functional Module Detection through Integration of Single-Cell RNA Sequencing Data with Protein–Protein Interaction Networks. *BMC Genomics* **21**, 756. ISSN: 1471-2164 (Nov. 2020).

49. Ridremont, T. *Design of Robust Networks. Application to the Design of Wind Farm Cabling Networks*. PhD thesis (Polytechnique Montréal, Apr. 2019). <https://publications.polymtl.ca/3889/> (Accessed on 03/02/2023).
50. Costa, A., Cordeau, J.-F. & Laporte, G. Steiner Tree Problems With Profits. *INFOR: Information Systems and Operational Research* **44**, 99–115. ISSN: 0315-5986 (May 2006).
51. Johnson, D. S., Minkoff, M. & Phillips, S. *The Prize Collecting Steiner Tree Problem: Theory and Practice* in *Proceedings of the Eleventh Annual ACM-SIAM Symposium on Discrete Algorithms* (Society for Industrial and Applied Mathematics, USA, Feb. 2000), 760–769. ISBN: 978-0-89871-453-1.
52. Haouari, M. & Chaouachi Siala, J. A Hybrid Lagrangian Genetic Algorithm for the Prize Collecting Steiner Tree Problem. *Computers & Operations Research* **33**, 1274–1288. ISSN: 0305-0548 (May 2006).
53. Álvarez-Miranda, E., Ljubić, I. & Toth, P. Exact Approaches for Solving Robust Prize-Collecting Steiner Tree Problems. *European Journal of Operational Research* **229**, 599–612. ISSN: 0377-2217 (Sept. 2013).
54. Leitner, M., Ljubić, I., Luipersbeck, M. & Sinnl, M. A Dual Ascent-Based Branch-and-Bound Framework for the Prize-Collecting Steiner Tree and Related Problems. *INFORMS Journal on Computing* **30**, 402–420. ISSN: 1091-9856 (May 2018).
55. Rehfeldt, D. & Koch, T. On the Exact Solution of Prize-Collecting Steiner Tree Problems. *INFORMS Journal on Computing* **34**, 872–889. ISSN: 1091-9856 (Mar. 2022).
56. Rehfeldt, D. & Koch, T. Implications, Conflicts, and Reductions for Steiner Trees. *Mathematical Programming* **197**, 903–966 (2023).
57. Wong, R. T. A Dual Ascent Approach for Steiner Tree Problems on a Directed Graph. *Mathematical Programming* **28**, 271–287. ISSN: 1436-4646 (Oct. 1984).
58. Goemans, M. & Myung, Y.-S. A Catalog of Steiner Tree Formulations. *Networks*. <https://www.semanticscholar.org/paper/A-catalog-of-steiners-tree-formulations-Goemans-Myung/5bd4c1df7446a9a217a2ee611df394292a4f8c48> (Accessed on 04/04/2023) (1993).
59. Ehrgott, M., Gandibleux, X. & Przybylski, A. in *Multiple Criteria Decision Analysis: State of the Art Surveys* (eds Greco, S., Ehrgott, M. & Figueira, J. R.) 817–850 (Springer, New York, NY, 2016). ISBN: 978-1-4939-3094-4.
60. Leitner, M., Ljubić, I. & Sinnl, M. A Computational Study of Exact Approaches for the Bi-Objective Prize-Collecting Steiner Tree Problem. *INFORMS Journal on Computing* **27**, 118–134. ISSN: 1091-9856 (Feb. 2015).
61. Takahashi, H. & Matsuyama, A. An Approximate Solution for the Steiner Problem in Graphs. *Mathematica Japonica*, 573–577 (1980).
62. Rehfeldt, D. *Faster Algorithms for Steiner Tree and Related Problems: From Theory to Practice* PhD thesis (Technische Universität Berlin, 2021). <https://opus4.kobv.de/opus4-zib/frontdoor/index/index/docId/8514> (Accessed on 02/24/2023).
63. Ryberg, D. S., Caglayan, D. G., Schmitt, S., Linßen, J., Stolten, D. & Robinius, M. The future of European onshore wind energy potential: Detailed distribution and simulation of advanced turbine designs. *Energy* **182**, 1222–1238. ISSN: 03605442 (2019).
64. OpenStreetMap contributors. *Overpass* 2021. <https://overpass-turbo.eu/> (Accessed on 09/29/2021).
65. Roth, M. in *Landschaftsplanung im Prozess und Dialog* (ed Marschall, I.) 114–126 (2018).
66. Gurobi Optimization, LLC. *Gurobi Optimizer Reference Manual, Version 9.5* 2022. <https://www.gurobi.com>.

67. Bestuzheva, K., Besançon, M., Chen, W.-K., Chmiela, A., Donkiewicz, T., van Doornmalen, J., Eifler, L., Gaul, O., Gamrath, G., Gleixner, A., Gottwald, L., Graczyk, C., Halbig, K., Hoen, A., Hojny, C., van der Hulst, R., Koch, T., Lübbecke, M., Maher, S. J., Matter, F., Mühmer, E., Müller, B., Pfetsch, M. E., Rehfeldt, D., Schlein, S., SchLÄÜsser, F., Serrano, F., Shinano, Y., Sofranac, B., Turner, M., Vigerske, S., Wegscheider, F., Wellner, P., Weninger, D. & Witzig, J. Enabling Research through the SCIP Optimization Suite 8.0. *ACM Transactions on Mathematical Software*. ISSN: 0098-3500. (Accessed on 04/18/2023) (Mar. 2023).
68. IBM ILOG. *V12.10: User's Manual for CPLEX 2022*. <https://www.ibm.com/analytics/cplex-optimizer>.
69. Spielhofer, R., Schwaab, J. & Grêt-Regamey, A. How spatial policies can leverage energy transitions Finding Pareto-optimal solutions for wind turbine locations with evolutionary multi-objective optimization. *Environmental Science & Policy* **142**, 220–232. ISSN: 1462-9011 (2023).
70. McKenna, R., Pfenninger, S., Heinrichs, H., Schmidt, J., Staffell, I., Bauer, C., Gruber, K., Hahmann, A. N., Jansen, M., Klingler, M., Landwehr, N., Larsén, X. G., Lilliestam, J., Pickering, B., Robinius, M., Tröndle, T., Turkovska, O., Wehrle, S., Weinand, J. M. & Wohland, J. High-resolution large-scale onshore wind energy assessments: A review of potential definitions, methodologies and future research needs. *Renewable Energy* **182**, 659–684. ISSN: 09601481 (2022).
71. McKenna, R., Mulalic, I., Soutar, I., Weinand, J., Price, J., Petrović, S. & Mainzer, K. Exploring trade-offs between landscape impact, land use and resource quality for onshore variable renewable energy: an application to Great Britain. *Energy* **250**, 123754 (2022).
72. Lehmann, P., Ammermann, K., Gawel, E., Geiger, C., Hauck, J., Heilmann, J., Meier, J.-N., Ponitka, J., Schicketanz, S., Stemmer, B., Tafarte, P., Thrän, D. & Wolfram, E. Managing spatial sustainability trade-offs: The case of wind power. *Ecological Economics* **185**, 107029. ISSN: 09218009 (2021).
73. McKenna, R., Bertsch, V., Mainzer, K. & Fichtner, W. Combining local preferences with multi-criteria decision analysis and linear optimization to develop feasible energy concepts in small communities. *European Journal of Operational Research* **268**. Community Operational Research: Innovations, internationalization and agenda-setting applications, 1092–1110 (2018).
74. Rehfeldt, D. & Koch, T. *Implications, Conflicts, and Reductions for Steiner Trees in Integer Programming and Combinatorial Optimization - 22nd International Conference, IPCO 2021, Atlanta, GA, USA, May 19-21, 2021, Proceedings* (eds Singh, M. & Williamson, D. P.) **12707** (Springer, 2021), 473–487.
75. Rehfeldt, D., Koch, T. & Maher, S. J. Reduction Techniques for the Prize Collecting Steiner Tree Problem and the Maximum-Weight Connected Subgraph Problem. *Networks* **73**, 206–233. ISSN: 1097-0037 (2019).
76. Fischetti, M., Fischetti, M. & Stoustrup, J. Safe distancing in the time of COVID-19. *European Journal of Operational Research* (2021).

A Detailed Computational Results

A.1 Region A

Table A.1: Detailed Results Region A

Quota	α	DB	PB	Gap [%]	Time [s]				
					GRB	QSTP	TQSTP	TQSTP+	TQSTP++
10.0	0.0	12.345		0.0	2.2	0.5	0.4	0.1	0.1
10.0	0.1	12.404		0.0	2.1	0.3	0.2	0.1	0.1
10.0	0.2	12.462		0.0	2.2	0.4	0.3	0.1	0.1
10.0	0.3	12.520		0.0	2.5	0.3	0.3	0.1	0.1
10.0	0.4	12.578		0.0	2.5	0.3	0.3	0.1	0.1
10.0	0.5	12.636		0.0	3.6	0.3	0.3	0.1	0.1
10.0	0.6	12.694		0.0	7.9	0.5	0.5	0.1	0.2
10.0	0.7	12.752		0.0	8.6	0.7	0.6	0.4	0.2
10.0	0.8	12.810		0.0	13.8	1.1	0.6	0.3	0.2
10.0	0.9	12.868		0.0	24.8	2.4	1.4	1.0	0.4
10.0	1.0	12.926		0.0	80.6	3.6	2.0	7.6	0.9
20.0	0.0	20.124		0.0	4.4	0.5	0.3	0.1	0.1
20.0	0.1	19.916		0.0	5.6	0.8	0.3	0.1	0.1
20.0	0.2	19.707		0.0	7.9	0.7	0.3	0.1	0.1
20.0	0.3	19.499		0.0	7.2	0.6	0.3	0.1	0.1
20.0	0.4	19.291		0.0	7.7	0.6	0.5	0.2	0.1
20.0	0.5	19.082		0.0	9.7	1.1	0.3	0.2	0.1
20.0	0.6	18.874		0.0	6.4	0.4	0.5	0.2	0.1
20.0	0.7	18.665		0.0	7.2	0.9	0.5	0.2	0.2
20.0	0.8	18.457		0.0	18.4	1.4	1.0	0.3	0.2
20.0	0.9	18.249		0.0	28.0	4.3	1.4	0.7	0.2
20.0	1.0	18.040		0.0	166.7	24.1	3.1	6.1	0.8
30.0	0.0	40.580		0.0	13.5	5.5	1.8	0.7	0.3
30.0	0.1	39.236		0.0	28.1	5.9	1.8	0.8	0.3
30.0	0.2	37.891		0.0	17.1	5.8	1.6	0.5	0.3
30.0	0.3	36.547		0.0	17.1	5.2	2.0	0.8	0.4
30.0	0.4	35.203		0.0	24.6	6.2	2.2	0.7	0.3
30.0	0.5	33.603		0.0	24.2	5.1	2.3	1.0	0.4
30.0	0.6	31.870		0.0	25.9	5.1	2.2	0.9	0.4
30.0	0.7	30.134		0.0	34.2	4.4	2.7	1.1	0.5
30.0	0.8	28.397		0.0	58.6	5.1	2.6	1.0	0.6
30.0	0.9	26.660		0.0	87.9	6.9	3.6	1.7	0.6
30.0	1.0	24.923		0.0	1103.5	14.0	4.1	8.7	2.3
40.0	0.0	55.945		0.0	26.6	5.7	1.9	0.6	0.4
40.0	0.1	54.086		0.0	23.9	6.7	2.6	0.8	0.3
40.0	0.2	52.226		0.0	23.8	7.3	2.0	1.4	0.4
40.0	0.3	50.367		0.0	26.2	3.5	3.4	1.0	0.4
40.0	0.4	48.507		0.0	40.2	13.6	4.0	1.3	0.4
40.0	0.5	46.393		0.0	54.1	12.8	5.0	2.2	0.5
40.0	0.6	44.145		0.0	60.0	14.4	3.9	1.5	0.4
40.0	0.7	41.893		0.0	91.5	16.8	2.9	1.4	0.6
40.0	0.8	39.206		0.0	180.0	27.1	4.1	1.9	0.9
40.0	0.9	35.635		0.0	256.6	30.1	5.6	1.9	1.8
40.0	1.0	31.938		0.0	786.5	48.8	9.1	7.0	3.5
50.0	0.0	68.268		0.0	23.8	1.5	1.1	0.4	0.1
50.0	0.1	65.688		0.0	26.3	1.9	1.1	0.4	0.2
50.0	0.2	63.109		0.0	28.4	2.1	1.4	0.5	0.1
50.0	0.3	60.530		0.0	26.8	2.2	1.3	0.5	0.1
50.0	0.4	57.950		0.0	38.7	2.7	1.4	0.6	0.2
50.0	0.5	55.116		0.0	45.3	2.8	3.2	0.8	0.2

Cont'd on next page

Table A.1: Detailed Results Region A – *Cont'd*

Quota	α	DB	PB	Gap [%]	Time [s]				
					GRB	QSTP	TQSTP	TQSTP+	TQSTP++
50.0	0.6	52.148		0.0	34.1	6.3	4.2	0.7	0.2
50.0	0.7	49.176		0.0	42.3	3.2	4.8	2.3	0.2
50.0	0.8	46.205		0.0	63.1	4.7	4.6	1.2	0.3
50.0	0.9	43.233		0.0	142.8	11.8	2.3	1.4	0.4
50.0	1.0	40.261		0.0	821.4	26.8	3.6	6.5	1.7
60.0	0.0	84.856		0.0	31.9	2.4	0.9	0.4	0.1
60.0	0.1	81.192		0.0	27.2	2.6	5.3	0.4	0.1
60.0	0.2	77.528		0.0	35.2	1.9	4.8	0.2	0.1
60.0	0.3	73.865		0.0	32.3	1.8	0.9	0.4	0.1
60.0	0.4	70.201		0.0	34.8	2.2	6.2	0.4	0.2
60.0	0.5	66.282		0.0	47.2	2.3	0.9	0.5	0.2
60.0	0.6	62.230		0.0	39.2	2.3	1.2	0.4	0.2
60.0	0.7	58.173		0.0	56.7	2.5	1.1	0.4	0.2
60.0	0.8	54.117		0.0	67.3	2.1	1.7	0.4	0.2
60.0	0.9	50.061		0.0	178.6	2.3	8.0	2.6	0.2
60.0	1.0	46.005		0.0	491.7	4.7	5.9	3.7	1.0
70.0	0.0	112.214		0.0	124.0	8.8	8.8	1.7	1.1
70.0	0.1	106.989		0.0	201.7	11.5	2.9	1.5	0.8
70.0	0.2	101.763		0.0	174.6	12.1	4.5	1.7	1.7
70.0	0.3	96.537		0.0	195.8	11.4	3.7	1.6	3.2
70.0	0.4	91.311		0.0	214.4	18.2	4.8	3.4	1.3
70.0	0.5	85.831		0.0	289.3	15.4	6.4	2.4	1.4
70.0	0.6	80.119		0.0	387.1	20.5	8.4	3.8	1.6
70.0	0.7	74.374		0.0	368.6	19.2	7.5	3.9	3.4
70.0	0.8	68.629		0.0	401.3	31.8	7.5	3.8	3.5
70.0	0.9	62.513		0.0	1357.3	99.4	13.8	7.6	6.9
70.0	1.0	54.949		0.0	2678.4	39.7	13.1	11.2	7.1
80.0	0.0	128.021		0.0	113.1	3.8	6.2	1.6	0.7
80.0	0.1	121.705		0.0	93.5	9.4	3.6	1.0	0.6
80.0	0.2	115.389		0.0	101.6	4.0	3.5	1.2	0.8
80.0	0.3	109.072		0.0	112.9	4.5	4.5	1.5	1.5
80.0	0.4	102.756		0.0	103.8	7.6	3.6	2.5	0.6
80.0	0.5	96.185		0.0	123.4	5.1	6.9	1.4	0.9
80.0	0.6	89.480		0.0	163.7	7.8	6.6	1.3	0.5
80.0	0.7	82.772		0.0	162.7	5.4	3.4	1.2	1.6
80.0	0.8	76.063		0.0	213.7	6.7	3.0	1.4	0.7
80.0	0.9	69.355		0.0	324.1	15.0	2.9	1.6	1.5
80.0	1.0	62.646		0.0	834.4	75.4	5.3	7.7	2.9
90.0	0.0	149.359		0.0	148.9	26.1	7.3	3.5	3.6
90.0	0.1	141.856		0.0	267.5	23.7	7.3	3.7	2.8
90.0	0.2	134.013		0.0	166.2	20.4	7.0	2.4	3.0
90.0	0.3	126.170		0.0	229.4	20.3	6.2	2.2	2.3
90.0	0.4	118.328		0.0	165.8	15.9	6.4	2.3	2.8
90.0	0.5	110.231		0.0	233.2	13.9	5.8	2.5	2.8
90.0	0.6	101.999		0.0	247.7	13.0	5.2	2.3	2.8
90.0	0.7	93.764		0.0	246.2	11.2	6.4	2.1	1.8
90.0	0.8	85.530		0.0	300.8	5.2	5.2	3.5	1.9
90.0	0.9	77.295		0.0	360.0	7.8	9.6	4.8	2.4
90.0	1.0	68.893		0.0	1495.4	5.7	5.3	5.2	2.9
100.0	0.0	164.134		0.0	68.7	6.2	6.2	1.7	0.9
100.0	0.1	155.758		0.0	89.3	4.6	3.5	1.5	0.7
100.0	0.2	147.381		0.0	76.8	6.5	5.0	1.8	0.7
100.0	0.3	139.005		0.0	85.6	6.3	2.4	0.9	0.7
100.0	0.4	130.628		0.0	111.3	17.6	2.2	0.9	0.8
100.0	0.5	121.997		0.0	80.0	7.5	2.4	0.9	0.9
100.0	0.6	113.232		0.0	105.2	12.1	3.0	1.1	0.7

Cont'd on next page

Table A.1: Detailed Results Region A – *Cont'd*

Quota	α	DB	PB	Gap [%]	Time [s]				
					GRB	QSTP	TQSTP	TQSTP+	TQSTP++
100.0	0.7	104.463		0.0	124.8	9.5	3.6	1.3	0.8
100.0	0.8	95.695		0.0	203.4	27.4	5.6	1.5	1.0
100.0	0.9	86.926		0.0	205.2	23.7	3.9	2.3	1.4
100.0	1.0	78.142		0.0	618.4	59.7	4.3	4.7	3.2
110.0	0.0	181.989		0.0	78.4	3.8	1.9	0.5	0.3
110.0	0.1	172.400		0.0	79.2	2.9	2.8	2.9	0.3
110.0	0.2	162.811		0.0	87.8	3.3	2.5	2.2	0.3
110.0	0.3	153.221		0.0	63.9	2.8	6.7	0.5	0.3
110.0	0.4	143.632		0.0	112.3	3.0	1.5	1.4	0.3
110.0	0.5	133.789		0.0	124.3	3.0	1.2	1.3	0.4
110.0	0.6	123.811		0.0	78.7	3.4	1.5	1.8	0.3
110.0	0.7	113.829		0.0	87.4	3.6	2.8	0.6	1.9
110.0	0.8	103.848		0.0	160.1	3.5	1.4	1.1	0.8
110.0	0.9	93.867		0.0	292.2	3.6	4.0	0.9	0.9
110.0	1.0	83.885		0.0	654.8	5.3	7.7	1.6	1.5
120.0	0.0	203.188		0.0	68.0	6.8	1.8	0.7	0.2
120.0	0.1	192.550		0.0	62.2	6.4	2.0	0.6	0.3
120.0	0.2	181.913		0.0	64.1	6.2	1.9	0.6	0.2
120.0	0.3	171.275		0.0	66.5	6.9	2.6	0.9	0.3
120.0	0.4	160.637		0.0	78.8	7.4	1.9	0.6	0.3
120.0	0.5	149.745		0.0	66.4	7.7	1.8	1.1	0.3
120.0	0.6	138.718		0.0	89.8	8.6	3.2	1.3	0.4
120.0	0.7	127.658		0.0	83.5	9.1	2.9	1.3	0.5
120.0	0.8	116.471		0.0	186.5	9.4	3.6	1.5	0.5
120.0	0.9	105.283		0.0	248.8	21.8	3.0	1.7	0.6
120.0	1.0	94.096		0.0	499.5	27.4	3.7	2.8	1.9
130.0	0.0	228.095		0.0	68.1	5.5	1.1	0.3	0.2
130.0	0.1	216.025		0.0	85.9	4.0	1.2	0.4	0.2
130.0	0.2	203.955		0.0	127.9	11.3	1.3	0.5	0.1
130.0	0.3	191.885		0.0	80.3	4.9	1.3	0.6	0.1
130.0	0.4	179.816		0.0	218.7	15.1	1.5	0.4	0.2
130.0	0.5	167.491		0.0	222.6	12.1	2.5	0.6	0.2
130.0	0.6	155.033		0.0	225.4	11.5	2.1	0.7	0.2
130.0	0.7	142.571		0.0	280.5	10.5	2.0	0.8	0.2
130.0	0.8	130.109		0.0	602.1	8.0	3.3	0.9	0.2
130.0	0.9	117.646		0.0	2890.7	11.5	4.6	2.1	0.8
130.0	1.0	102.034		0.0	2240.0	11.2	4.6	4.3	3.0
140.0	0.0	270.846		0.0	243.4	12.2	2.7	0.9	0.2
140.0	0.1	255.802		0.0	436.1	12.6	3.2	0.7	0.2
140.0	0.2	240.759		0.0	396.8	13.2	2.9	0.7	0.2
140.0	0.3	225.715		0.0	659.4	12.0	2.7	0.8	0.2
140.0	0.4	210.672		0.0	649.1	13.7	3.3	0.9	0.3
140.0	0.5	195.374		0.0	1304.3	14.3	3.0	1.1	0.3
140.0	0.6	179.635		0.0	1798.7	13.9	3.5	1.6	0.5
140.0	0.7	162.938		0.0	939.6	13.8	3.5	1.0	0.5
140.0	0.8	146.115		0.0	1743.4	14.1	3.0	0.8	0.7
140.0	0.9	129.291		0.0	1890.8	14.3	2.5	1.0	0.6
140.0	1.0	112.456		0.0	1583.8	19.0	3.0	2.1	1.8
150.0	0.0	315.185		0.0	1470.0	9.8	2.8	0.9	0.6
150.0	0.1	296.403		0.0	1838.8	10.6	2.5	0.8	0.5
150.0	0.2	277.621		0.0	678.6	10.9	2.8	1.2	0.6
150.0	0.3	258.840		0.0	1196.8	10.1	3.0	0.9	0.5
150.0	0.4	240.058		0.0	927.7	16.2	2.7	1.1	0.6
150.0	0.5	221.021		0.0	1830.7	11.4	3.0	1.1	0.7
150.0	0.6	201.851		0.0	1592.1	13.2	3.1	1.2	0.7
150.0	0.7	182.677		0.0	2684.9	12.4	3.1	1.4	0.6

Cont'd on next page

Table A.1: Detailed Results Region A – *Cont'd*

Quota	α	DB	PB	Gap [%]	Time [s]				
					GRB	QSTP	TQSTP	TQSTP+	TQSTP++
150.0	0.8	163.503		0.0	1813.0	13.0	3.1	1.4	0.9
150.0	0.9	144.329		0.0	1738.4	14.8	3.0	1.8	0.9
150.0	1.0	125.143		0.0	2659.4	20.6	3.3	3.0	1.6
158.0	0.0	333.875		0.0	521.5	6.4	2.5	0.8	0.4
158.0	0.1	313.831		0.0	491.4	6.2	2.7	0.7	0.5
158.0	0.2	293.786		0.0	496.2	6.5	3.1	0.7	0.5
158.0	0.3	273.742		0.0	384.2	6.7	3.1	0.8	0.5
158.0	0.4	253.698		0.0	514.1	6.3	3.0	0.9	0.4
158.0	0.5	233.399		0.0	648.4	6.8	2.8	0.9	0.5
158.0	0.6	212.965		0.0	687.9	6.4	3.1	0.8	0.5
158.0	0.7	192.529		0.0	481.6	7.0	2.7	1.1	0.6
158.0	0.8	172.092		0.0	464.1	6.9	3.1	1.2	0.7
158.0	0.9	151.656		0.0	567.9	8.5	2.8	1.3	0.8
158.0	1.0	130.974		0.0	707.3	6.1	2.9	2.9	1.2

A.2 Region B

Table A.2: Detailed Results Region B

Quota	α	TQSTP				TQSTP+				TQSTP++			
		DB	PB	Gap [%]	t [s]	DB	PB	Gap [%]	t [s]	DB	PB	Gap [%]	t [s]
50.0	0.1	83.4	–	–	21600	96.8	110.8	14.5	1336	109.5	0.0	–	477
50.0	0.1	78.0	1572.9	1915.9	21600	103.0	–	0.0	1042	103.0	0.0	–	314
50.0	0.2	73.0	1346.3	1744.2	15035	96.4	–	0.0	480	96.4	0.0	–	227
50.0	0.3	69.2	–	–	21600	89.8	–	0.0	1307	89.8	0.0	–	173
50.0	0.4	69.6	199.4	186.4	21600	83.3	–	0.0	1205	83.3	0.0	–	348
50.0	0.5	–	76.7	0.0	11552	76.7	–	0.0	2523	76.7	0.0	–	417
50.0	0.6	55.5	–	–	21600	70.1	–	0.0	1231	70.1	0.0	–	278
50.0	0.7	50.5	–	–	21600	63.6	–	0.0	1122	63.6	0.0	–	350
50.0	0.8	48.4	161.9	234.2	21600	57.0	–	0.0	930	57.0	0.0	–	599
50.0	0.9	41.0	–	–	21600	49.6	–	0.0	6053	49.6	0.0	–	1033
50.0	1.0	35.9	–	–	21600	37.3	–	–	21600	41.9	0.0	–	1051
100.0	0.0	172.5	–	–	21600	208.7	–	0.0	1259	208.7	0.0	–	423
100.0	0.1	162.9	–	–	21600	196.7	–	0.0	2098	196.7	0.0	–	311
100.0	0.2	156.4	981.8	527.6	21600	184.6	–	0.0	2580	184.6	0.0	–	402
100.0	0.3	143.3	–	–	21600	162.2	–	–	21600	172.5	0.0	–	395
100.0	0.4	132.9	–	–	21600	160.5	–	0.0	1057	160.5	0.0	–	355
100.0	0.5	123.4	–	–	21600	148.4	–	0.0	2646	148.4	0.0	–	553
100.0	0.6	112.9	–	–	21600	136.3	–	0.0	945	136.3	0.0	–	1116
100.0	0.7	102.1	–	–	21600	122.9	–	0.0	3773	122.9	0.0	–	742
100.0	0.8	91.3	–	–	21600	100.7	–	–	21600	109.0	0.0	–	1096
100.0	0.9	80.5	–	–	21600	89.4	363.6	306.6	21600	95.0	0.0	–	1111
100.0	1.0	69.1	–	–	21600	73.1	–	–	21600	81.1	0.0	–	4833
150.0	0.0	265.3	–	–	21600	320.7	–	0.0	9823	320.7	0.0	–	789
150.0	0.1	251.0	–	–	21600	301.6	–	0.0	3570	301.6	0.0	–	833
150.0	0.2	234.5	–	–	21600	282.5	–	0.0	5149	282.5	0.0	–	1050
150.0	0.3	219.5	–	–	21600	263.4	–	0.0	7616	263.4	0.0	–	1903
150.0	0.4	203.9	–	–	21600	244.3	–	0.0	6396	244.3	0.0	–	1872
150.0	0.5	188.7	–	–	21600	225.2	–	0.0	6034	225.2	0.0	–	1719
150.0	0.6	172.8	–	–	21600	206.1	–	0.0	11309	199.5	208.5	4.5	7530
150.0	0.7	156.9	–	–	21600	182.0	186.6	2.5	13160	183.5	186.6	1.7	21600
150.0	0.8	141.4	–	–	21600	162.5	165.8	2.0	21600	165.1	0.0	–	4638
150.0	0.9	125.6	–	–	21600	135.9	354.4	160.7	21600	143.1	0.0	–	2387
150.0	1.0	109.4	–	–	21600	113.0	413.4	266.0	21600	121.1	0.0	–	5498
175.0	0.0	320.2	493.1	54.0	21600	369.7	–	0.0	4325	369.7	0.0	–	645
175.0	0.1	295.1	–	–	21600	347.4	–	0.0	4773	347.4	0.0	–	1239
175.0	0.2	277.2	–	–	21600	325.0	–	0.0	1603	325.0	0.0	–	641
175.0	0.3	259.4	–	–	21600	302.7	–	0.0	5488	302.7	0.0	–	1189
175.0	0.4	240.2	–	–	21600	280.4	–	0.0	9486	280.4	0.0	–	1383
175.0	0.5	222.5	–	–	21600	258.0	–	0.0	6351	258.0	0.0	–	817
175.0	0.6	203.8	–	–	21600	235.7	–	0.0	1959	235.7	0.0	–	1186
175.0	0.7	185.5	–	–	21600	212.8	–	0.0	2050	212.8	0.0	–	1594
175.0	0.8	167.2	–	–	21600	180.1	–	–	21600	189.8	0.0	–	2107
175.0	0.9	147.8	–	–	21600	166.7	–	0.0	18947	166.7	0.0	–	4484
175.0	1.0	127.4	–	–	21600	131.8	–	–	21600	132.9	147.1	10.8	13431
200.0	0.0	362.9	–	–	21600	430.2	–	0.0	3113	430.2	0.0	–	2112
200.0	0.1	341.6	–	–	21600	404.0	–	0.0	2156	404.0	0.0	–	2337
200.0	0.2	320.0	–	–	21600	377.7	–	0.0	6314	377.7	0.0	–	1819
200.0	0.3	299.7	–	–	21600	351.4	–	0.0	3114	351.4	0.0	–	1130
200.0	0.4	278.9	–	–	21600	325.1	–	0.0	9165	325.1	0.0	–	1262
200.0	0.5	257.7	–	–	21600	298.9	–	0.0	4115	298.9	0.0	–	3430
200.0	0.6	235.9	–	–	21600	272.6	–	0.0	17641	272.6	0.0	–	4160
200.0	0.7	214.7	–	–	21600	245.8	–	0.0	12690	245.8	0.0	–	5335

Cont'd on next page

Table A.2: Detailed Results Region B – *Cont'd*

Quota	α	TQSTP				TQSTP+				TQSTP++			
		DB	PB	Gap [%]	t [s]	DB	PB	Gap [%]	t [s]	DB	PB	Gap [%]	t [s]
200.0	0.8	192.0	–	–	21600	218.8	–	0.0	6748	218.8	–	0.0	10080
200.0	0.9	169.7	–	–	21600	189.5	197.7	4.3	21600	182.2	198.2	8.7	20007
200.0	1.0	147.4	–	–	21600	151.2	–	–	21600	152.2	173.6	14.1	10092
250.0	0.0	466.6	–	–	21600	558.5	–	0.0	7387	553.2	561.5	1.5	6530
250.0	0.1	438.8	–	–	21600	525.0	–	0.0	7512	525.0	–	0.0	5945
250.0	0.2	412.9	–	–	21600	486.3	490.5	0.9	21600	490.5	–	0.0	3371
250.0	0.3	384.3	–	–	21600	455.9	–	0.0	7190	455.9	–	0.0	2468
250.0	0.4	356.5	–	–	21600	414.9	440.5	6.2	21600	421.3	–	0.0	5757
250.0	0.5	329.8	–	–	21600	386.7	–	0.0	16469	386.7	–	0.0	10711
250.0	0.6	301.0	–	–	21600	352.1	–	0.0	11010	352.1	–	0.0	4298
250.0	0.7	273.1	–	–	21600	316.9	–	0.0	14757	316.9	–	0.0	12084
250.0	0.8	245.1	–	–	21600	281.3	–	0.0	12567	279.4	281.3	0.7	21600
250.0	0.9	216.9	–	–	21600	232.0	247.0	6.5	21600	231.5	250.5	8.2	16919
250.0	1.0	188.9	–	–	21600	192.9	–	–	21600	192.8	217.0	12.6	12943
300.0	0.0	583.6	–	–	21600	684.7	690.9	0.9	21600	689.8	–	0.0	11340
300.0	0.1	548.0	–	–	21600	644.3	648.5	0.7	21600	648.3	–	0.0	9264
300.0	0.2	513.9	–	–	21600	594.8	2075.8	249.0	21600	603.7	606.0	0.4	21600
300.0	0.3	477.8	–	–	21600	560.4	563.3	0.5	21600	563.3	–	0.0	14187
300.0	0.4	443.8	–	–	21600	520.7	–	0.0	20849	520.7	–	0.0	9732
300.0	0.5	408.9	–	–	21600	450.7	486.5	7.9	6578	450.8	487.8	8.2	9643
300.0	0.6	373.8	–	–	21600	410.8	–	–	21600	431.2	442.6	2.6	18148
300.0	0.7	339.0	–	–	21600	387.5	401.3	3.5	21600	391.5	–	0.0	12673
300.0	0.8	303.6	–	–	21600	327.1	–	–	21600	347.8	–	0.0	15987
300.0	0.9	267.8	–	–	21600	294.8	525.2	78.2	21600	303.9	–	0.0	16408
300.0	1.0	232.2	–	–	21600	236.6	–	–	21600	236.3	269.5	14.0	9232
350.0	0.0	702.3	–	–	21600	827.7	–	0.0	10382	827.7	–	0.0	7662
350.0	0.1	660.4	–	–	21600	777.2	–	0.0	6855	777.2	–	0.0	4750
350.0	0.2	619.8	–	–	21600	723.3	726.5	0.4	21600	726.5	–	0.0	6513
350.0	0.3	577.5	–	–	21600	642.5	690.4	7.4	11482	675.8	–	0.0	9842
350.0	0.4	534.9	–	–	21600	625.1	–	0.0	19053	625.1	–	0.0	12418
350.0	0.5	493.1	–	–	21600	567.7	1534.4	170.3	21600	572.3	588.1	2.8	19545
350.0	0.6	450.7	–	–	21600	523.7	–	0.0	20440	521.7	523.7	0.4	21600
350.0	0.7	407.3	–	–	21600	446.4	–	–	21600	467.4	472.5	1.1	21600
350.0	0.8	365.2	–	–	21600	414.9	445.6	7.4	21600	414.6	430.4	3.8	21600
350.0	0.9	322.2	–	–	21600	344.7	–	–	21600	364.1	381.8	4.9	21600
350.0	1.0	279.2	–	–	21600	283.0	–	–	21600	283.9	322.6	13.6	18054
405.0	0.0	863.3	–	–	21600	1035.3	–	0.0	5232	1035.3	–	0.0	2990
405.0	0.1	811.3	–	–	21600	970.6	–	0.0	5617	970.6	–	0.0	4173
405.0	0.2	759.5	–	–	21600	905.7	–	0.0	9853	905.7	–	0.0	3168
405.0	0.3	708.6	–	–	21600	840.8	–	0.0	6346	840.8	–	0.0	3108
405.0	0.4	656.1	–	–	21600	775.9	–	0.0	6496	775.9	–	0.0	4787
405.0	0.5	604.1	–	–	21600	711.0	–	0.0	9200	711.0	–	0.0	5637
405.0	0.6	551.9	–	–	21600	613.4	–	–	21600	646.0	–	0.0	5631
405.0	0.7	499.4	–	–	21600	579.9	–	0.0	21221	579.9	–	0.0	6635
405.0	0.8	447.9	–	–	21600	485.8	–	–	21600	513.1	–	0.0	9293
405.0	0.9	395.3	–	–	21600	426.0	503.1	18.1	21600	445.9	–	0.0	13983
405.0	1.0	343.7	–	–	21600	345.9	–	–	21600	347.4	379.0	9.1	19463

B Best Results by Costs and Scenicness

B.1 Region A

Table B.3: Cost and scenicness in each instance of region A

Quota	α	$\sum q$	$\sum c$	$\sum s$	Gap [%]
10	0.0	14.4	12.93	12.35	0.0
10	0.1	14.4	12.93	12.35	0.0
10	0.2	14.4	12.93	12.35	0.0
10	0.3	14.4	12.93	12.35	0.0
10	0.4	14.4	12.93	12.35	0.0
10	0.5	14.4	12.93	12.35	0.0
10	0.6	14.4	12.93	12.35	0.0
10	0.7	14.4	12.93	12.35	0.0
10	0.8	14.4	12.93	12.35	0.0
10	0.9	14.4	12.93	12.35	0.0
10	1.0	14.4	12.93	12.35	0.0
20	0.0	21.1	18.04	20.12	0.0
20	0.1	21.1	18.04	20.12	0.0
20	0.2	21.1	18.04	20.12	0.0
20	0.3	21.1	18.04	20.12	0.0
20	0.4	21.1	18.04	20.12	0.0
20	0.5	21.1	18.04	20.12	0.0
20	0.6	21.1	18.04	20.12	0.0
20	0.7	21.1	18.04	20.12	0.0
20	0.8	21.1	18.04	20.12	0.0
20	0.9	21.1	18.04	20.12	0.0
20	1.0	21.1	18.04	20.12	0.0
30	0.0	30.0	27.14	40.58	0.0
30	0.1	30.0	27.14	40.58	0.0
30	0.2	30.0	27.14	40.58	0.0
30	0.3	30.0	27.14	40.58	0.0
30	0.4	30.0	27.14	40.58	0.0
30	0.5	30.0	24.95	42.26	0.0
30	0.6	30.0	24.92	42.29	0.0
30	0.7	30.0	24.92	42.29	0.0
30	0.8	30.0	24.92	42.29	0.0
30	0.9	30.0	24.92	42.29	0.0
30	1.0	30.0	24.92	42.29	0.0
40	0.0	43.1	37.35	55.95	0.0
40	0.1	43.1	37.35	55.95	0.0
40	0.2	43.1	37.35	55.95	0.0
40	0.3	43.1	37.35	55.95	0.0
40	0.4	43.1	37.35	55.95	0.0
40	0.5	43.1	35.16	57.63	0.0
40	0.6	43.1	35.14	57.66	0.0
40	0.7	43.1	35.14	57.66	0.0
40	0.8	40.3	32.19	67.27	0.0
40	0.9	40.3	32.04	68.00	0.0
40	1.0	40.3	31.94	69.32	0.0
50	0.0	51.6	42.47	68.27	0.0
50	0.1	51.6	42.47	68.27	0.0
50	0.2	51.6	42.47	68.27	0.0
50	0.3	51.6	42.47	68.27	0.0
50	0.4	51.6	42.47	68.27	0.0
50	0.5	51.6	40.28	69.95	0.0
50	0.6	51.6	40.26	69.98	0.0

Cont'd on next page

Table B.3 – *Cont'd*

Quota	α	$\sum q$	$\sum c$	$\sum s$	Gap [%]
50	0.7	51.6	40.26	69.98	0.0
50	0.8	51.6	40.26	69.98	0.0
50	0.9	51.6	40.26	69.98	0.0
50	1.0	51.6	40.26	69.98	0.0
60	0.0	60.8	48.22	84.86	0.0
60	0.1	60.8	48.22	84.86	0.0
60	0.2	60.8	48.22	84.86	0.0
60	0.3	60.8	48.22	84.86	0.0
60	0.4	60.8	48.22	84.86	0.0
60	0.5	60.8	46.03	86.54	0.0
60	0.6	60.8	46.00	86.57	0.0
60	0.7	60.8	46.00	86.57	0.0
60	0.8	60.8	46.00	86.57	0.0
60	0.9	60.8	46.00	86.57	0.0
60	1.0	60.8	46.00	86.57	0.0
70	0.0	70.4	59.96	112.21	0.0
70	0.1	70.4	59.96	112.21	0.0
70	0.2	70.4	59.96	112.21	0.0
70	0.3	70.4	59.96	112.21	0.0
70	0.4	70.4	59.96	112.21	0.0
70	0.5	70.4	57.77	113.89	0.0
70	0.6	71.8	57.14	114.59	0.0
70	0.7	71.8	57.14	114.59	0.0
70	0.8	71.8	57.14	114.59	0.0
70	0.9	70.1	55.35	126.99	0.0
70	1.0	70.1	54.95	132.25	0.0
80	0.0	80.4	64.86	128.02	0.0
80	0.1	80.4	64.86	128.02	0.0
80	0.2	80.4	64.86	128.02	0.0
80	0.3	80.4	64.86	128.02	0.0
80	0.4	80.4	64.86	128.02	0.0
80	0.5	80.4	62.67	129.70	0.0
80	0.6	80.4	62.65	129.73	0.0
80	0.7	80.4	62.65	129.73	0.0
80	0.8	80.4	62.65	129.73	0.0
80	0.9	80.4	62.65	129.73	0.0
80	1.0	80.4	62.65	129.73	0.0
90	0.0	91.0	74.92	149.36	0.0
90	0.1	90.7	71.27	149.70	0.0
90	0.2	90.7	71.27	149.70	0.0
90	0.3	90.7	71.27	149.70	0.0
90	0.4	90.7	71.27	149.70	0.0
90	0.5	90.7	69.08	151.38	0.0
90	0.6	90.7	69.06	151.41	0.0
90	0.7	90.7	69.06	151.41	0.0
90	0.8	90.7	69.06	151.41	0.0
90	0.9	90.7	69.06	151.41	0.0
90	1.0	90.1	68.89	157.68	0.0
100	0.0	100.2	80.37	164.13	0.0
100	0.1	100.2	80.37	164.13	0.0
100	0.2	100.2	80.37	164.13	0.0
100	0.3	100.2	80.37	164.13	0.0
100	0.4	100.2	80.37	164.13	0.0
100	0.5	100.2	78.18	165.81	0.0
100	0.6	100.2	78.16	165.84	0.0
100	0.7	100.2	78.16	165.84	0.0
100	0.8	100.2	78.16	165.84	0.0

Cont'd on next page

Table B.3 – *Cont'd*

Quota	α	$\sum q$	$\sum c$	$\sum s$	Gap [%]
100	0.9	100.2	78.16	165.84	0.0
100	1.0	101.4	78.14	167.11	0.0
110	0.0	110.5	86.10	181.99	0.0
110	0.1	110.5	86.10	181.99	0.0
110	0.2	110.5	86.10	181.99	0.0
110	0.3	110.5	86.10	181.99	0.0
110	0.4	110.5	86.10	181.99	0.0
110	0.5	110.5	83.91	183.67	0.0
110	0.6	110.5	83.89	183.70	0.0
110	0.7	110.5	83.89	183.70	0.0
110	0.8	110.5	83.89	183.70	0.0
110	0.9	110.5	83.89	183.70	0.0
110	1.0	110.5	83.89	183.70	0.0
120	0.0	120.7	96.81	203.19	0.0
120	0.1	120.7	96.81	203.19	0.0
120	0.2	120.7	96.81	203.19	0.0
120	0.3	120.7	96.81	203.19	0.0
120	0.4	120.7	96.81	203.19	0.0
120	0.5	120.7	94.62	204.87	0.0
120	0.6	120.7	94.60	204.90	0.0
120	0.7	122.4	94.10	205.97	0.0
120	0.8	122.4	94.10	205.97	0.0
120	0.9	122.4	94.10	205.97	0.0
120	1.0	122.4	94.10	205.97	0.0
130	0.0	133.4	107.40	228.09	0.0
130	0.1	133.4	107.40	228.09	0.0
130	0.2	133.4	107.40	228.09	0.0
130	0.3	133.4	107.40	228.09	0.0
130	0.4	133.4	107.40	228.09	0.0
130	0.5	133.4	105.21	229.77	0.0
130	0.6	133.4	105.18	229.80	0.0
130	0.7	133.4	105.18	229.80	0.0
130	0.8	133.4	105.18	229.80	0.0
130	0.9	133.4	105.18	229.80	0.0
130	1.0	131.4	102.03	258.16	0.0
140	0.0	143.5	120.41	270.85	0.0
140	0.1	143.5	120.41	270.85	0.0
140	0.2	143.5	120.41	270.85	0.0
140	0.3	143.5	120.41	270.85	0.0
140	0.4	143.5	120.41	270.85	0.0
140	0.5	143.5	118.22	272.53	0.0
140	0.6	140.7	112.97	279.63	0.0
140	0.7	142.4	112.47	280.70	0.0
140	0.8	142.4	112.47	280.70	0.0
140	0.9	142.4	112.47	280.70	0.0
140	1.0	142.4	112.46	281.41	0.0
150	0.0	152.6	127.37	315.18	0.0
150	0.1	152.6	127.37	315.18	0.0
150	0.2	152.6	127.37	315.18	0.0
150	0.3	152.6	127.37	315.18	0.0
150	0.4	152.6	127.37	315.18	0.0
150	0.5	152.6	125.18	316.87	0.0
150	0.6	152.6	125.15	316.90	0.0
150	0.7	152.6	125.15	316.90	0.0
150	0.8	152.6	125.15	316.90	0.0
150	0.9	152.6	125.15	316.90	0.0
150	1.0	152.6	125.14	317.61	0.0

Cont'd on next page

Table B.3 – *Cont'd*

Quota	α	$\sum q$	$\sum c$	$\sum s$	Gap [%]
158	0.0	158.4	133.43	333.88	0.0
158	0.1	158.4	133.43	333.88	0.0
158	0.2	158.4	133.43	333.88	0.0
158	0.3	158.4	133.43	333.88	0.0
158	0.4	158.4	133.43	333.88	0.0
158	0.5	158.4	131.24	335.56	0.0
158	0.6	158.4	131.22	335.59	0.0
158	0.7	158.4	131.22	335.59	0.0
158	0.8	158.4	131.22	335.59	0.0
158	0.9	158.4	131.22	335.59	0.0
158	1.0	158.4	130.97	338.82	0.0

B.2 Region B

Table B.4: Cost and scenicness in each instance of region B

Quota	α	$\sum q$	$\sum c$	$\sum s$	Gap [%]
50	0.0	50.1	43.85	109.52	0.0
50	0.1	50.1	43.85	109.52	0.0
50	0.2	50.1	43.85	109.52	0.0
50	0.3	50.1	43.85	109.52	0.0
50	0.4	50.1	43.85	109.52	0.0
50	0.5	50.1	43.85	109.52	0.0
50	0.6	50.1	43.85	109.52	0.0
50	0.7	50.1	43.85	109.52	0.0
50	0.8	50.1	43.85	109.52	0.0
50	0.9	52.4	41.92	118.92	0.0
50	1.0	52.4	41.92	118.96	0.0
100	0.0	100.1	88.09	208.72	0.0
100	0.1	100.1	88.09	208.72	0.0
100	0.2	100.1	88.09	208.72	0.0
100	0.3	100.1	88.09	208.72	0.0
100	0.4	100.1	88.08	208.72	0.0
100	0.5	100.1	88.08	208.72	0.0
100	0.6	100.1	88.08	208.72	0.0
100	0.7	101.7	81.12	220.29	0.0
100	0.8	101.7	81.12	220.29	0.0
100	0.9	101.7	81.12	220.29	0.0
100	1.0	101.7	81.12	220.29	0.0
150	0.0	151.4	129.79	320.67	0.0
150	0.1	151.4	129.79	320.67	0.0
150	0.2	151.4	129.79	320.67	0.0
150	0.3	151.4	129.79	320.67	0.0
150	0.4	151.4	129.79	320.67	0.0
150	0.5	151.4	129.79	320.67	0.0
150	0.6	150.5	127.24	330.49	4.5
150	0.7	150.2	124.14	332.25	1.7
150	0.8	150.3	121.14	341.03	0.0
150	0.9	150.3	121.14	341.03	0.0
150	1.0	150.3	121.10	342.89	0.0
175	0.0	175.2	146.36	369.71	0.0
175	0.1	175.2	146.36	369.71	0.0
175	0.2	175.2	146.36	369.71	0.0
175	0.3	175.2	146.36	369.71	0.0
175	0.4	175.2	146.35	369.71	0.0
175	0.5	175.2	146.35	369.71	0.0
175	0.6	175.2	146.33	369.74	0.0
175	0.7	175.2	143.71	374.09	0.0
175	0.8	175.2	143.71	374.09	0.0
175	0.9	175.1	143.64	374.45	0.0
175	1.0	175.3	147.13	411.56	10.8
200	0.0	200.2	167.51	430.23	0.0
200	0.1	200.2	167.51	430.23	0.0
200	0.2	200.2	167.51	430.23	0.0
200	0.3	200.2	167.51	430.23	0.0
200	0.4	200.2	167.51	430.23	0.0
200	0.5	200.2	167.51	430.23	0.0
200	0.6	200.2	167.51	430.23	0.0
200	0.7	200.2	164.78	434.74	0.0
200	0.8	200.2	164.78	434.74	0.0
200	0.9	200.8	169.20	458.78	8.7

Cont'd on next page

Table B.4 – *Cont'd*

Quota	α	$\sum q$	$\sum c$	$\sum s$	Gap [%]
200	1.0	200.0	173.65	480.55	14.1
250	0.0	250.3	212.83	561.45	1.5
250	0.1	250.1	223.38	558.47	0.0
250	0.2	250.5	213.62	559.76	0.0
250	0.3	250.5	213.62	559.76	0.0
250	0.4	250.5	213.62	559.76	0.0
250	0.5	250.5	213.55	559.81	0.0
250	0.6	250.5	213.55	559.81	0.0
250	0.7	250.3	210.10	565.96	0.0
250	0.8	250.3	210.10	565.98	0.7
250	0.9	250.6	213.38	585.07	8.2
250	1.0	250.5	216.99	593.21	12.6
300	0.0	300.3	275.83	689.80	0.0
300	0.1	300.3	273.14	689.97	0.0
300	0.2	300.2	265.03	691.19	0.4
300	0.3	300.2	265.03	691.19	0.0
300	0.4	300.2	263.26	692.30	0.0
300	0.5	300.2	263.43	712.24	8.2
300	0.6	300.0	263.48	711.16	2.6
300	0.7	300.2	260.46	697.31	0.0
300	0.8	300.3	260.25	697.88	0.0
300	0.9	301.0	260.01	699.07	0.0
300	1.0	300.0	269.46	758.80	14.0
350	0.0	350.1	323.69	827.66	0.0
350	0.1	350.1	321.00	827.84	0.0
350	0.2	350.1	321.00	827.84	0.0
350	0.3	350.1	321.00	827.84	0.0
350	0.4	350.1	321.00	827.84	0.0
350	0.5	351.4	325.03	851.10	2.8
350	0.6	350.1	317.98	833.40	0.4
350	0.7	350.1	317.83	833.32	1.1
350	0.8	350.3	321.57	865.91	3.8
350	0.9	350.1	323.87	903.39	4.9
350	1.0	353.4	322.56	911.39	13.6
405	0.0	405.7	389.60	1035.28	0.0
405	0.1	405.7	386.91	1035.45	0.0
405	0.2	405.7	386.61	1035.49	0.0
405	0.3	405.7	386.61	1035.49	0.0
405	0.4	405.7	386.61	1035.49	0.0
405	0.5	405.7	386.04	1035.92	0.0
405	0.6	405.7	386.04	1035.92	0.0
405	0.7	405.7	381.08	1043.81	0.0
405	0.8	405.7	378.75	1050.57	0.0
405	0.9	405.7	378.71	1050.81	0.0
405	1.0	405.7	379.02	1053.31	9.1